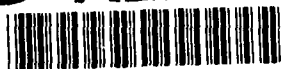


2

NAVAL POSTGRADUATE SCHOOL Monterey, California

AD-A274 921



DTIC
ELECTE
JAN 25 1994
S E D

THESIS

A FINITE WAKE THEORY
FOR TWO-DIMENSIONAL ROTARY WING
UNSTEADY AERODYNAMICS

by

Mark A. Couch

September, 1993

Thesis Advisor:

E. Roberts Wood

Approved for public release; distribution is unlimited.

94 1 25 003

94-02106

REPORT DOCUMENTATION PAGE			Form Approved OMB No. 0704-
Public reporting burden for this collection of information is estimated to average 1 hour per response, including the time for reviewing instruction, searching existing data sources, gathering and maintaining the data needed, and completing and reviewing the collection of information. Send comments regarding this burden estimate or any other aspect of this collection of information, including suggestions for reducing this burden, to Washington headquarters Services, Directorate for Information Operations and Reports, 1215 Jefferson Davis Highway, Suite 1204, Arlington, VA 22202-4302, and to the Office of Management and Budget, Paperwork Reduction Project (0704-0188) Washington DC 20503.			
1. AGENCY USE ONLY (Leave blank)	2. REPORT DATE 23 September 1993	3. REPORT TYPE AND DATES COVERED Master's Thesis	
4. TITLE AND SUBTITLE A FINITE WAKE THEORY FOR TWO-DIMENSIONAL ROTARY WING UNSTEADY AERODYNAMICS		5. FUNDING NUMBERS	
6. AUTHOR(S) Mark A. Couch		8. PERFORMING ORGANIZATION REPORT NUMBER	
7. PERFORMING ORGANIZATION NAME(S) AND ADDRESS(ES) Naval Postgraduate School Monterey CA 93943-5000		10. SPONSORING/MONITORING AGENCY REPORT NUMBER	
9. SPONSORING/MONITORING AGENCY NAME(S) AND ADDRESS(ES)		11. SUPPLEMENTARY NOTES The views expressed in this thesis are those of the author and do not reflect the official policy or position of the Department of Defense or the U.S. Government.	
12a. DISTRIBUTION/AVAILABILITY STATEMENT Approved for public release; distribution is unlimited.		12b. DISTRIBUTION CODE A	
13. ABSTRACT (maximum 200 words) <p>The unsteady aerodynamic forces and moments of an oscillating airfoil for the fixed wing case were determined by Theodorsen along with the development of a lift deficiency function. Loewy subsequently developed an analogous lift deficiency function for the rotary wing case in which there are an infinite number of layers of shed vorticity, or wakes, below the reference airfoil. With the advent of computer panel codes that calculate the time histories of the wakes generated by oscillating airfoils, a theory is developed for the rotary wing case in which there are a finite number of layers of shed vorticity below the reference airfoil. This theory includes a lift deficiency function that is completely analogous to Loewy and Theodorsen.</p> <p>It has long been recognized that an airfoil oscillating in pure plunge produces a propulsive force ("Katzmayr effect"). Garrick used Theodorsen's work to develop equations for the propulsive force that include the lift deficiency function as a parameter. When either Loewy's lift deficiency function or the finite wake lift deficiency function is used, the effect of the propulsive force is greatly enhanced with the proper phase relationship of the wakes. The finite wake theory along with Garrick's work is used to describe the performance characteristics of Higher Harmonic Control. Specifically for the OH-6A, coupled pitch-plunge motion results in a propulsive force that significantly reduces the rotor drag force.</p>			
14. SUBJECT TERMS Helicopter, Rotary Wing, Unsteady Aerodynamics, Wake, Propulsive Force, Higher Harmonic Control, Hummingbird			15. NUMBER OF PAGES 69
			16. PRICE CODE
17. SECURITY CLASSIFICATION OF REPORT Unclassified	18. SECURITY CLASSIFICATION OF THIS PAGE Unclassified	19. SECURITY CLASSIFICATION OF ABSTRACT Unclassified	20. LIMITATION OF ABSTRACT UL

NSN 7540-01-280-5500

Standard Form 298 (Rev. 2-89)

Prescribed by ANSI Std. Z39-18

Approved for public release; distribution is unlimited.

Accession For	
NTIS CRA&I	<input checked="" type="checkbox"/>
DTIC TAB	<input checked="" type="checkbox"/>
Unannounced	<input type="checkbox"/>
Justification	
By	
Distribution /	
Availability Codes	
Dist	Avail and/or Special
A-1	

A Finite Wake Theory
For Two-Dimensional Rotary Wing
Unsteady Aerodynamics

by

Mark A. Couch
Lieutenant, United States Navy
B.S., Purdue University, 1984

Submitted in partial fulfillment
of the requirements for the degree of

MASTER OF SCIENCE IN AERONAUTICAL ENGINEERING

from the

NAVAL POSTGRADUATE SCHOOL

September 1993

Author:

Mark A. Couch

Mark A. Couch

Approved by:

E. Roberts Wood

E. Roberts Wood, Thesis Advisor

Max F. Platzer

Max F. Platzer, Second Reader

Daniel J. Collins

Daniel J. Collins, Chairman

Department of Aeronautics and Astronautics

ABSTRACT

The unsteady aerodynamic forces and moments of an oscillating airfoil for the fixed wing case were determined by Theodorsen along with the development of a lift deficiency function. Loewy subsequently developed an analogous lift deficiency function for the rotary wing case in which there are an infinite number of layers of shed vorticity, or wakes, below the reference airfoil. With the advent of computer panel codes that calculate the time histories of the wakes generated by oscillating airfoils, a theory is developed for the rotary wing case in which there are a finite number of layers of shed vorticity below the reference airfoil. This theory includes a lift deficiency function that is completely analogous to Loewy and Theodorsen.

It has long been recognized that an airfoil oscillating in pure plunge produces a propulsive force ("Katzmayr effect"). Garrick used Theodorsen's work to develop equations for the propulsive force that include the lift deficiency function as a parameter. When either Loewy's lift deficiency function or the finite wake lift deficiency function is used, the effect of the propulsive force is greatly enhanced with the proper phase relationship of the wakes. The finite wake theory along with Garrick's work is used to describe the performance characteristics of Higher Harmonic Control. Specifically for the OH-6A, coupled pitch-plunge motion results in a propulsive force that significantly reduces the rotor drag force.

TABLE OF CONTENTS

I. INTRODUCTION	1
A. GENERAL	1
B. SCOPE	2
II. BACKGROUND	3
A. THEODORSEN'S LIFT DEFICIENCY FUNCTION	3
B. GARRICK'S PROPULSIVE FORCE EQUATION	10
III. ANALYSIS	14
A. LOEWY'S LIFT DEFICIENCY FUNCTION	14
B. FINITE WAKE LIFT DEFICIENCY FUNCTION	26
1. General	26
2. Single Wake Case	31
3. Multiple Wake Case	39
IV. APPLICATIONS	42
A. EXTENSIONS AND COMPARISON OF THEORY	42
1. Forward Airspeed	42
2. Compressibility Effects	43

3. NPS Unsteady Panel Code	44
B. HIGHER HARMONIC CONTROL	44
V. CONCLUSION	51
APPENDIX A	53
I. FLIGHT OF THE HUMMINGBIRD	53
LIST OF REFERENCES	56
INITIAL DISTRIBUTION LIST	58

TABLE C F SYMBOLS

a	non-dimensional elastic axis location measured from midchord
A	mathematical expression denoting group of terms described by equation (61)
A_N	mathematical expression denoting group of terms described by equation (77)
b	semichord length
B	mathematical expression denoting group of terms described by equation (62)
B_N	mathematical expression denoting group of terms described by equation (78)
C(k)	Theodorsen's lift deficiency function, $C(k) = F + iG$
C'(k)	Loewy's lift deficiency function, $C'(k) = F' + iG'$
C*(k)	finite wake lift deficiency function, $C^*(k) = F^* + iG^*$
C_{px}	propulsive force coefficient
F	real part of Theodorsen's lift deficiency function
F'	real part of Loewy's lift deficiency function
F*	real part of finite wake lift deficiency function
G	imaginary part of Theodorsen's lift deficiency function
G'	imaginary part of Loewy's lift deficiency function
G*	imaginary part of finite wake lift deficiency function
h	non-dimensional distance between layers of shed vorticity (wake spacing)
	$h = \frac{2\pi v}{bQ\Omega}$
h	simple harmonic motion of vertical deflection, $h = h_0 e^{i\omega t}$

- h_o amplitude of deflection in simple harmonic motion of $h_o e^{i\omega t}$ (plunge)
- \bar{h}_o non-dimensional amplitude of deflection, $\bar{h}_o = \frac{h_o}{b}$
- \dot{h} first derivative with respect to time of vertical deflection motion (plunge)
- \ddot{h} second derivative with respect to time of vertical deflection motion (plunge)
- $H_n^{(2)}$ Hankel function (complex Bessel function) of second kind of order n ,

$$H_n^{(2)} = J_n + Y_n$$
- i complex notation, $i = \sqrt{-1}$
- J_n real part of complex Bessel function of order n
- k reduced frequency, $k = \frac{\omega b}{v}$
- m ratio of oscillation frequency to rotational frequency, $m = \frac{\omega}{\Omega}$
- M_a aerodynamic moment about the elastic axis (positive clockwise)
- n revolution number
- N number of rotor revolutions (reduces to the number of wakes for single-blade rotor)
- Δp pressure difference across airfoil
- \bar{P}_x propulsive force
- q blade number
- Q total number of rotor blades
- r blade section radius
- S x-component of induced downwash velocity
- t time
- U vortex distribution per unit length

v	freestream velocity
V	forward airspeed
w	downwash velocity
W	Loewy's wake weighting function
W_N	finite wake weighting function
x	non-dimensional distance from midchord
x_o	non-dimensional distance from midchord
Y_n	imaginary part of complex Bessel function
α	simple harmonic motion of pitch angle, $\alpha = \alpha_o e^{i\omega t}$
α_o	amplitude of rotation in simple harmonic motion of $\alpha_o e^{i\omega t}$
$\dot{\alpha}$	first derivative with respect to time of rotation motion (pitch)
$\ddot{\alpha}$	second derivative with respect to time of rotation motion (pitch)
$\hat{\alpha}$	real part of Loewy's wake weighting function
$\hat{\alpha}_N$	real part of finite wake weighting function
$\hat{\beta}$	imaginary part of Loewy's wake weighting function
$\hat{\beta}_N$	imaginary part of finite wake weighting function
γ_s	vorticity generated by reference airfoil
γ_{nq}	vorticity generated by q th blade in n th revolution
Γ	total circulation around airfoil
μ	advance ratio, $\mu = \frac{V}{\Omega r}$
ξ	non-dimensional distance from midchord
ρ	density of air

Φ, φ velocity potentials

φ_0 phase angle between initiation of rotation input and arbitrary reference point

φ_2 phase angle between initiation of amplitude input and arbitrary reference point

ψ_q phase angle by which motion of q th blade leads reference blade

ω frequency of oscillation

Ω rotational frequency of rotor

ACKNOWLEDGEMENTS

I would like to give my sincere appreciation to Dr. E. Roberts Wood for his guidance, encouragement, and many hours of discussion that led to the completion of this project. I would like to thank Dr. Max F. Platzer whose knowledge of unsteady aerodynamics was of great assistance to me.

I would like to thank LTC Ahmed Abourahma of Egypt for his work on Dr. Platzer's panel code. Without the work on the panel code, my theory for finite wakes might not have come into fruition. I would also like to thank the staff and faculty in the Department of Aeronautics and Astronautics for making this an enjoyable two years.

I would like to give my deepest thanks to my lovely wife, Pam, for her encouragement and support throughout my time here and over nine years of marriage. Finally, to my daughters, Kelsey and Amy, you are too young to understand now the gift I was given by being able to see you two each day instead of being deployed somewhere. That gift I will always treasure.

I. INTRODUCTION

A. GENERAL

The present knowledge of rotary wing unsteady aerodynamics is limited. The fundamental closed form solutions by Theodorsen [Ref. 1] and Loewy [Ref. 2] provide the basis for the theoretical work in this area. While Loewy's work on wake-induced flutter helps explain the phenomenon, it also points out the difficulty to be overcome which is the closed form theory shows rapid changes in the lift deficiency function with changes in reduced frequency (k), wake spacing (h), and frequency ratio (m).

In the past, emphasis in the study of unsteady aerodynamics has tended to focus on flutter instability and the effects of unsteady aerodynamics on lift generation and torsional loads, and not on performance. In this thesis, the emphasis will be on performance and the effect of unsteady aerodynamics on the drag of the airfoil. The classic work on this subject was performed by Garrick [Ref. 3]. In this work, Garrick found that the drag force could be reversed, acting to propel the airfoil forward. This drag reversal is generally referred to as either negative drag or propulsive force.

The primary objective of this thesis is twofold. First, the effect of rotary wing unsteady aerodynamics on the drag of an airfoil will be analyzed. It will be shown that this effect can be either substantially greater than that shown by Garrick, or substantially less depending on the frequency ratio (m). This change in the effect is due to layers of shed vorticity (or wakes) below the rotor blades. Second, with the

recent advent of computer panel codes capable of calculating the time histories of the wakes generated by oscillating airfoils, a closed form theory is developed for the rotary wing aerodynamics in which there are a finite number of wakes below the rotor blades. It will be shown that this theory is completely analogous to Theodorsen and Loewy's work, and applicable to Garrick's work.

B. SCOPE

Chapter II is a short review of the work of Theodorsen [Ref. 1] and Garrick [Ref. 3]. The material is presented in a manner to allow one to understand the key assumptions made in each theory without being overcome by the details. Chapter III contains an analysis of Loewy's work [Ref. 2] and applies it to Garrick. The closed form finite wake theory is also presented here, as well as the special case of a single wake. Chapter IV is a limited discussion on applications of finite wake rotary wing unsteady aerodynamic theory. The first section discusses logical extensions of this theory to include forward airspeed [Ref. 4] and compressibility effects [Ref. 5 and 6]. A comparison of this theory to the Naval Postgraduate School (NPS) Unsteady Panel Code [Ref. 7 and 8] for the case of pure plunge is also included in the first section. The second section presents an explanation for the performance benefits due to Higher Harmonic Control (HHC). Appendix A is another application of this theory describing the efficient nature of flight of the hummingbird. The discussions in Chapter IV and Appendix A are not designed to provide all the answers to the questions arising from these applications. They are designed to show that positive performance effects can be found in the application of rotary wing unsteady aerodynamics.

II. BACKGROUND

A. THEODORSEN'S LIFT DEFICIENCY FUNCTION

The aerodynamic forces and moments on an oscillating airfoil for the fixed-wing case as determined by Theodorsen [Ref. 1] are based on potential flow theory and the Kutta condition. Potential flow theory reduces to Laplace's equation for the case of incompressible subsonic flow.

$$\frac{\partial^2 \Phi}{\partial x^2} + \frac{\partial^2 \Phi}{\partial y^2} = 0 \quad (1)$$

Since potential flow theory follows the principle of superposition, the potentials can be treated as two types: non-circulatory and circulatory. The non-circulatory terms are *primarily from the effects* of the freestream with the airfoil. The circulatory terms result from the vorticity generated in the wake of the airfoil. It is in the circulatory terms that the lift deficiency function is defined.

The aerodynamic forces and moments on a thin airfoil, depicted in Figure 1, are obtained by integrating the pressure difference across the airfoil determined from the generalized Bernoulli equation as follows:

$$P = b \int_{-1}^1 p(x) dx \quad (2)$$

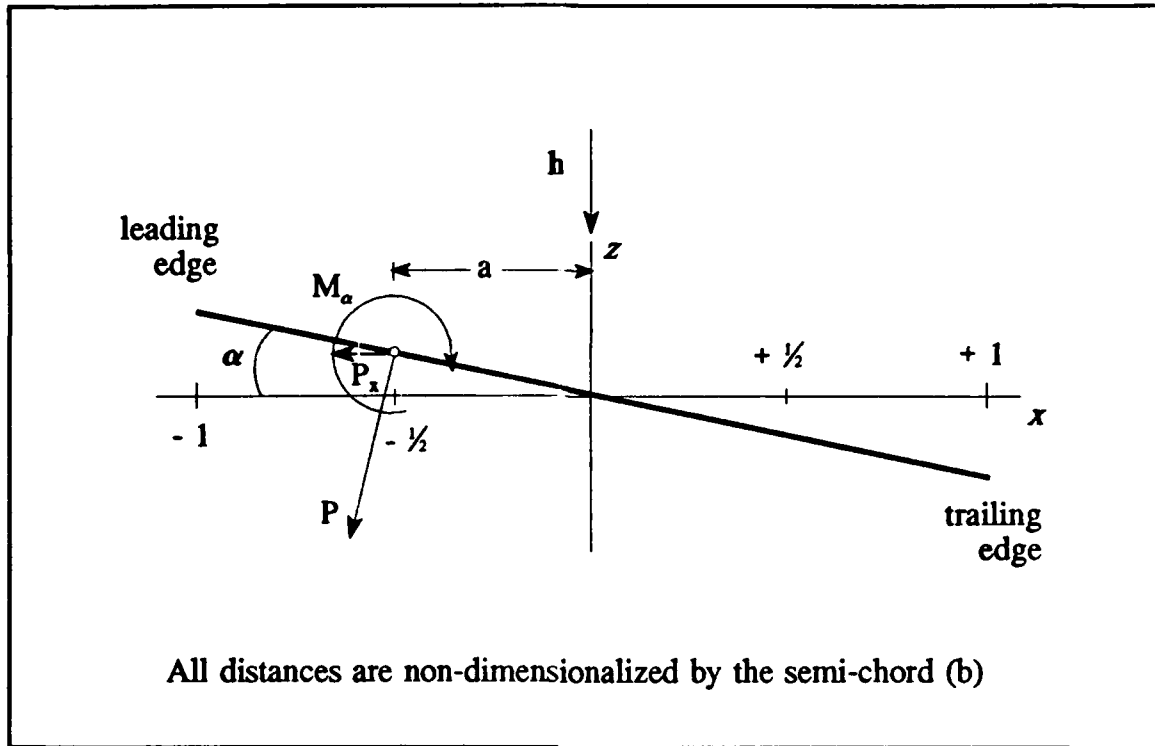


Figure 1. Parameters of the thin airfoil.

and

$$M_a = b^2 \int_{-1}^1 p(x)(x-a) dx , \quad (3)$$

where the generalized Bernoulli equation is written as

$$\Delta p(x) = -2\rho \left(\frac{v}{b} \frac{\partial \phi}{\partial x} + \frac{\partial \phi}{\partial t} \right) . \quad (4)$$

In the manner suggested by Scanlan and Rosenbaum [Ref. 9], the potential flow for the non-circulatory terms can be written as

$$\varphi_N = \frac{b w(\xi)}{2\pi} \log \left[\frac{1 - x\xi - \sqrt{1-x^2}\sqrt{1-\xi^2}}{1 - x\xi + \sqrt{1-x^2}\sqrt{1-\xi^2}} \right]. \quad (5)$$

The pressure difference across the airfoil for the non-circulatory terms is

$$\begin{aligned} \Delta p(x)_N = & \frac{-2\rho v}{\pi\sqrt{1-x^2}} \int_{-1}^1 \frac{\sqrt{1-\xi^2}}{x-\xi} w(\xi) d\xi \\ & - \frac{i\omega\rho b}{\pi} \int_{-1}^1 \log \left[\frac{1 - x\xi - \sqrt{1-x^2}\sqrt{1-\xi^2}}{1 - x\xi + \sqrt{1-x^2}\sqrt{1-\xi^2}} \right] w(\xi) d\xi, \end{aligned} \quad (6)$$

where the downwash¹ $w(\xi) = \dot{h} + b(\xi-a)\dot{\alpha} + v\alpha$, and simple harmonic motion is assumed, or $w = w_0 e^{i\omega t}$. Integrating the pressure difference in equation (6) to obtain the non-circulatory forces and moments yields

$$P_N = -\pi\rho b^2(v\dot{\alpha} + \dot{h} - ba\ddot{\alpha}) \quad (7)$$

and

$$(M_\alpha)_N = -\pi\rho b^2 \left[\left(\frac{1}{2} - a \right) v b \dot{\alpha} + b^2 \left(\frac{1}{8} + a^2 \right) \ddot{\alpha} - a b \dot{h} \right]. \quad (8)$$

The potentials of the circulatory terms are determined by integrating the velocity potential resulting from a single vortex element with a vortex distribution per unit length, $U(x_0)$, that is assumed to vary sinusoidally. This yields a circulation potential of

¹Only two degrees of freedom (pitch and plunge) are presented here since most rotary wing aircraft do not have ailerons incorporated on the rotor blades.

$$\Phi_{\Gamma} = \int_1^{\infty} d\varphi_{\Gamma} = \int_1^{\infty} \frac{U(x_o) b}{2\pi} \tan^{-1} \left[\frac{\sqrt{1-x^2} \sqrt{x_o^2-1}}{1-x-x_o} \right] dx_o. \quad (9)$$

The Kutta condition, which requires the velocity at the trailing edge to be finite, can be written as

$$\left(\frac{\partial \varphi_N}{\partial x} \right)_{\text{edge}} + \left(\frac{\partial \Phi_{\Gamma}}{\partial x} \right)_{\text{edge}} = \text{finite}. \quad (10)$$

This results in

$$w(\xi) \sqrt{\frac{1+\xi}{1-\xi}} d\xi = -\frac{1}{2} \int_1^{\infty} U(x_o) \frac{x_o+1}{\sqrt{x_o^2-1}} dx_o. \quad (11)$$

Now defining a lift deficiency function as

$$C(k) = \frac{\int_1^{\infty} \frac{x_o}{\sqrt{x_o^2-1}} e^{-ikx_o} dx_o}{\int_1^{\infty} \frac{x_o+1}{\sqrt{x_o^2-1}} e^{-ikx_o} dx_o}, \quad (12)$$

the Kutta condition becomes

$$-2w(\xi) d\xi \sqrt{\frac{1+\xi}{1-\xi}} C(k) = \int_1^{\infty} \frac{x_o U(x_o)}{\sqrt{x_o^2-1}} dx_o. \quad (13)$$

Using equation (4) the pressure difference across the airfoil for the circulatory terms is

$$\Delta p(x)_\Gamma = \frac{2\rho v}{\pi\sqrt{1-x^2}} \left\{ C(k) + x[1 - C(k)] \right\} \int_{-1}^1 \sqrt{\frac{1+\xi}{1-\xi}} w(\xi) d\xi . \quad (14)$$

Integrating the pressure difference in equation (14) to obtain the circulatory forces and moments yields

$$P_\Gamma = -2\pi\rho vbC(k) \left[v\alpha + \dot{h} + b\left(\frac{1}{2} - a\right)\dot{\alpha} \right] \quad (15)$$

and

$$(M_\alpha)_\Gamma = 2\pi\rho vb^2 \left(a + \frac{1}{2} \right) C(k) \left[v\alpha + \dot{h} + b\left(\frac{1}{2} - a\right)\dot{\alpha} \right] . \quad (16)$$

The total pressure difference is obtained by adding the pressure differences for the non-circulatory and circulatory terms. After some algebraic manipulation the total unsteady pressure distribution can be written as

$$\begin{aligned} -\frac{\Delta p(x)}{\rho v} = & \frac{2}{\pi} [1 - C(k)] \int_{-1}^1 \sqrt{\frac{1-x}{1+x}} \sqrt{\frac{1+\xi}{1-\xi}} w(\xi) d\xi \\ & + \frac{2}{\pi} \int_{-1}^1 \left[\sqrt{\frac{1-x}{1+x}} \sqrt{\frac{1+\xi}{1-\xi}} \left(\frac{1}{x-\xi} \right) \right. \\ & \left. - \frac{ik}{2} \log \left(\frac{1-x\xi - \sqrt{1-x^2}\sqrt{1-\xi^2}}{1-x\xi + \sqrt{1-x^2}\sqrt{1-\xi^2}} \right) \right] w(\xi) d\xi . \end{aligned} \quad (17)$$

Likewise the total forces and moments are obtained by adding their two parts together yielding

$$P = -\pi\rho b^2 (v\dot{\alpha} + \dot{h} - ba\ddot{\alpha}) - 2\pi\rho vbC(k) \left[v\alpha + \dot{h} + b\left(\frac{1}{2} - a\right)\dot{\alpha} \right] \quad (18)$$

and

$$M_a = -\pi \rho b^2 \left[\left(\frac{1}{2} - a \right) v L_1 + L_2 \left(\frac{1}{8} + a^2 \right) \ddot{\alpha} - a b \ddot{h} \right] + 2\pi \rho v b^2 \left(\frac{1}{2} - a \right) C(k) \left[v \alpha + \dot{h} + b \left(\frac{1}{2} - a \right) \dot{\alpha} \right]. \quad (19)$$

The analytical solution to the lift deficiency function involves the use of complex Bessel functions (or Hankel functions), and can be written as

$$C(k) = \frac{H_1^{(2)}}{H_1^{(2)} + iH_0^{(2)}}, \quad (20)$$

where $H_n^{(2)} = J_n - iY_n$ is the Hankel function of the second kind of order n . The lift deficiency function can be separated into its real and imaginary parts as

$$C(k) = F(k) + iG(k), \quad (21)$$

where

$$F(k) = \frac{J_1(J_1 + Y_0) + Y_1(Y_1 - J_0)}{(J_1 + Y_0)^2 + (Y_1 - J_0)^2} \quad (22)$$

and

$$G(k) = -\frac{Y_1 Y_0 + J_1 J_0}{(J_1 + Y_0)^2 + (Y_1 - J_0)^2}, \quad (23)$$

and all Bessel functions are evaluated at the reduced frequency (k). A typical plot of $F(k)$ and $G(k)$ as given by Theodorsen [Ref. 1], is shown in Figure 2. Figure 3 is a semi-logarithmic plot of Theodorsen's lift deficiency function, and the limits of $F(k)$

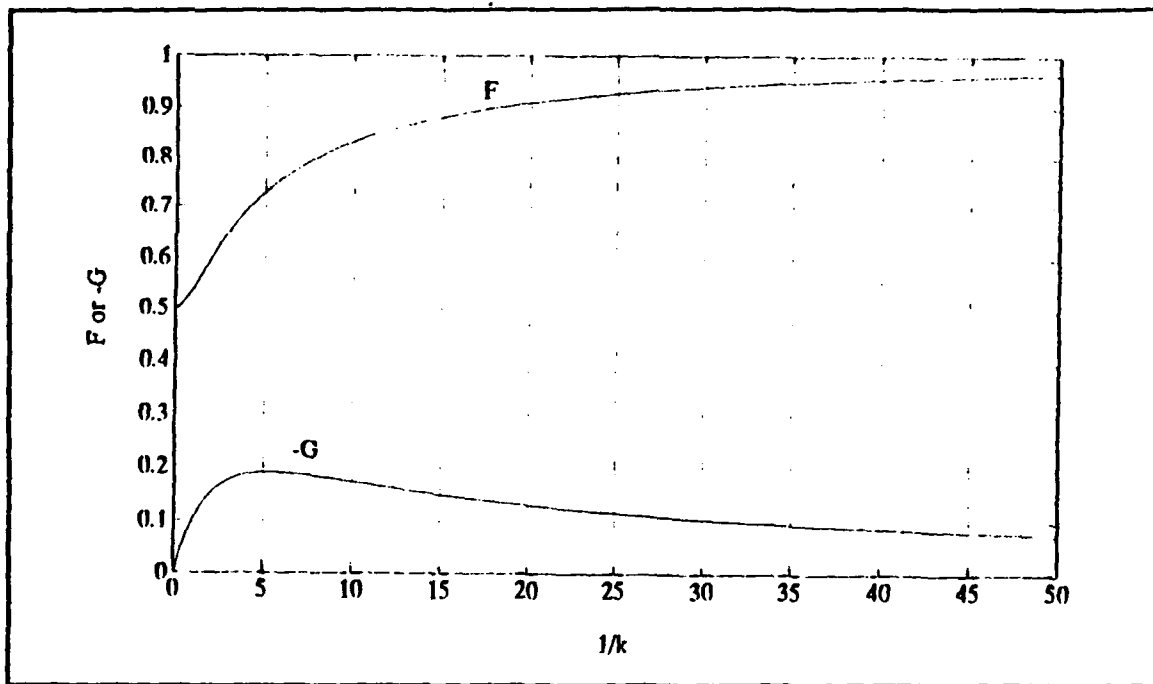


Figure 2. Conventional plot of Theodorsen's lift deficiency function.

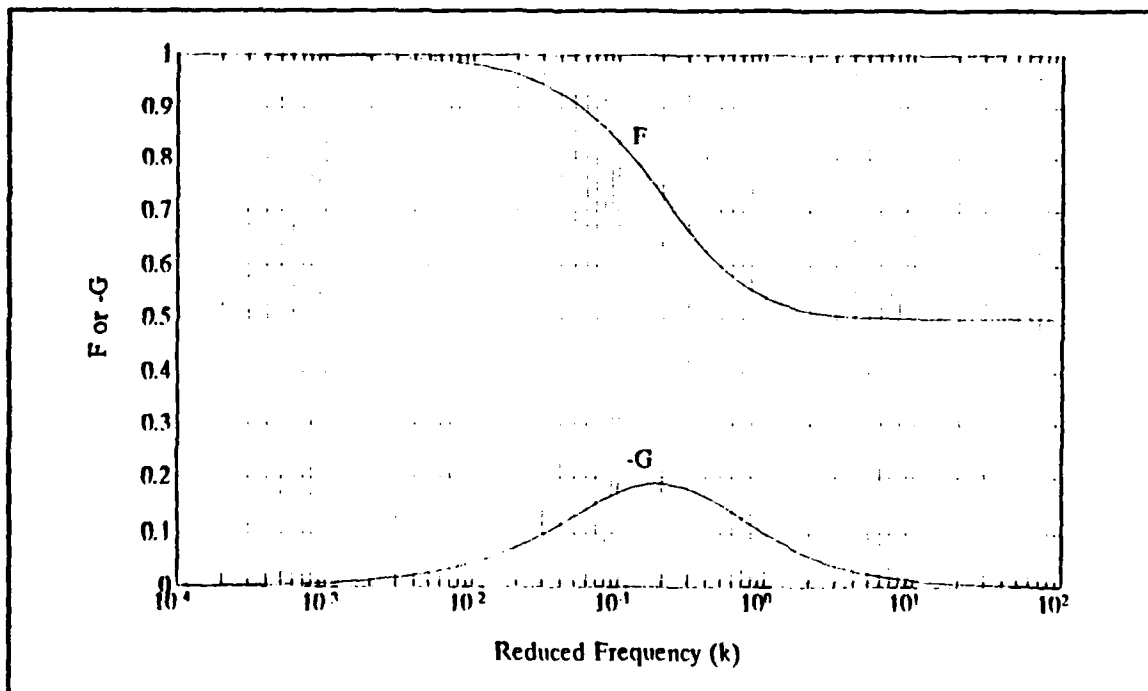


Figure 3. Semi-logarithmic plot of Theodorsen's lift deficiency function.

and $G(k)$ as k approaches zero and infinity can be more easily seen. It is an interesting note that when $\frac{\partial G}{\partial k} = 0$, $k = -G = 0.188773655....$

B. GARRICK'S PROPULSIVE FORCE EQUATION

One of the earliest investigations on the effect of an oscillating airfoil on the resultant drag was conducted by Katzmayr [Ref. 10] in two series of experiments. In his second series, Katzmayr measured a negative drag or propulsive force for certain velocities and frequencies. This discovery, later to be known as the "Katzmayr effect", helped answer questions on how birds propel themselves through the air. Richardson [Ref. 11] used the "Katzmayr effect" to explain the locomotion of fish through the water. Garrick [Ref. 3] applied the equations of motion determined by Theodorsen [Ref. 1], equations (18) and (19), to a method developed by von Karman and Burgers [Ref. 12] to obtain a closed form analytical solution for the propulsive force generated by an oscillating airfoil.²

Garrick determines the average horizontal force by two methods: energy and force. He then compares the results of these methods, and shows they are identical. For simplicity only the force method is presented here. First he assumes simple harmonic motion for each of the degrees of freedom, resulting in

$$\alpha = \alpha_0 e^{i(\omega t + \phi_0)} \quad (24)$$

²Though Garrick developed his equations for three degrees of freedom, only two degrees of freedom (pitch and plunge) will be presented here.

and

$$h = h_0 e^{i(\omega t + \varphi_2)} , \quad (25)$$

where φ_0 and φ_2 are phase angles between the initiation of the input and an arbitrary reference point.

The total horizontal force on the airfoil is given by

$$P_x = \pi \rho S^2 + \alpha P \quad (26)$$

where P_x is the propulsive force on the airfoil (positive to the left), P is the resultant force on the airfoil (positive down), and S is the component of induced downwash in the x-direction. The time averaged propulsive force is found by

$$\bar{P}_x = \frac{\omega}{2\pi} \int_0^{2\pi/\omega} P_x dt . \quad (27)$$

The x-component of the induced downwash is

$$S = \frac{1}{\sqrt{2}} \left\{ 2C(k) \left[v\alpha + \dot{h} + b \left(\frac{1}{2} - a \right) \dot{\alpha} \right] - b\dot{\alpha} \right\} . \quad (28)$$

In finding the solution to the time averaged propulsive force equation, it is arbitrary whether one chooses to employ the real or imaginary parts; the results will be the same. Garrick [Ref. 3] chose the imaginary parts, and determined the time averaged propulsive force to be

$$\begin{aligned}
\bar{P}_x = \pi \rho b \omega^2 & \left\{ h_o^2 (F^2 + G^2) \right. \\
& + b^2 \alpha_o^2 \left[(F^2 + G^2) \left(\frac{1}{k^2} + \left(\frac{1}{2} - a \right)^2 \right) + \frac{1}{2} \left(\frac{1}{2} - a \right) - F \left(\frac{1}{2} - a + \frac{1}{k^2} \right) - \frac{G}{k} \left(a + \frac{1}{2} \right) \right] \\
& + b \alpha_o h_o \left[\left(\frac{1}{k} (F^2 + G^2) + \frac{F}{2k} + \frac{G}{2} \right) \sin(\varphi_2 - \varphi_o) \right. \\
& \left. \left. + \left(\left(\frac{1}{2} - a \right) (F^2 + G^2) + \frac{1}{2} \left(\frac{1}{2} - \frac{G}{k} - F \right) \right) \cos(\varphi_2 - \varphi_o) \right] \right\} .
\end{aligned} \tag{29}$$

It is interesting to note that in the special cases of only one degree of freedom, the effects of the arbitrary phase angles between initiation and the reference point disappear. The propulsive force equations become for pure plunge ($\alpha_o = 0$)

$$\bar{P}_x = \pi \rho b \omega^2 h_o^2 (F^2 + G^2) , \tag{30}$$

and for pure pitch ($h_o = 0$)³

$$\begin{aligned}
\bar{P}_x = \pi \rho b \omega^2 b^2 \alpha_o^2 & \left\{ (F^2 + G^2) \left[\frac{1}{k^2} + \left(\frac{1}{2} - a \right)^2 \right] + \frac{1}{2} \left(\frac{1}{2} - a \right) \right. \\
& \left. - F \left(\frac{1}{2} - a + \frac{1}{k^2} \right) - \left(\frac{1}{2} + a \right) \frac{G}{k} \right\} .
\end{aligned} \tag{31}$$

If it is assumed that pitch and plunge are in phase with each other (they reach their maximum deflections at the same time), the coupled propulsive force equation becomes

³The result presented here differs from Garrick's equation (34) in reference 3. When equation (29) in reference 3 is simplified using the definitions of a_2 and b_2 , the result is equation (31) above. This result has been confirmed by Garrick's work in reference 10.

$$\begin{aligned}\bar{P}_x = & \pi \rho b \omega^2 \left\{ h_o^2 (F^2 + G^2) \right. \\ & + b^2 \alpha_o^2 \left[(F^2 + G^2) \left(\frac{1}{k^2} + \left(\frac{1}{2} - a \right)^2 \right) + \frac{1}{2} \left(\frac{1}{2} - a \right) - F \left(\frac{1}{2} - a + \frac{1}{k^2} \right) - \left(\frac{1}{2} + a \right) \frac{G}{k} \right] \\ & \left. + b \alpha_o h_o \left[\left(\frac{1}{2} - a \right) (F^2 + G^2) + \frac{1}{2} \left(\frac{1}{2} - \frac{G}{k} - F \right) \right] \right\}. \quad (32)\end{aligned}$$

Since propulsive force is analogous to negative drag, it is convenient to define a propulsive force coefficient as

$$C_{P_x} = \frac{\bar{P}_x}{\frac{1}{2} \rho v^2 (2b)} = \frac{\bar{P}_x}{\rho v^2 b}. \quad (33)$$

The propulsive force coefficients for the special cases become for pure plunge ($\alpha_o = 0$)

$$C_{P_x} = \pi k^2 \bar{h}_o^2 (F^2 + G^2), \quad (34)$$

where \bar{h}_o is the amplitude of deflection non-dimensionalized by the semi-chord, for pure pitch ($h_o = 0$)

$$C_{P_x} = \pi k^2 \alpha_o^2 \left\{ (F^2 + G^2) \left[\frac{1}{k^2} + \left(\frac{1}{2} - a \right)^2 \right] + \frac{1}{2} \left(\frac{1}{2} - a \right) - F \left(\frac{1}{2} - a + \frac{1}{k^2} \right) - \left(\frac{1}{2} + a \right) \frac{G}{k} \right\}, \quad (35)$$

and for coupled pitch and plunge

$$\begin{aligned}C_{P_x} = & \pi k^2 \left\{ \bar{h}_o^2 (F^2 + G^2) + \alpha_o^2 \left[(F^2 + G^2) \left(\frac{1}{k^2} + \left(\frac{1}{2} - a \right)^2 \right) + \frac{1}{2} \left(\frac{1}{2} - a \right) \right. \right. \\ & \left. \left. - F \left(\frac{1}{2} - a + \frac{1}{k^2} \right) - \left(\frac{1}{2} + a \right) \frac{G}{k} \right] + \alpha_o \bar{h}_o \left[\left(\frac{1}{2} - a \right) (F^2 + G^2) + \frac{1}{2} \left(\frac{1}{2} - \frac{G}{k} - F \right) \right] \right\}. \quad (36)\end{aligned}$$

III ANALYSIS

A. LOEWY'S LIFT DEFICIENCY FUNCTION

The aerodynamic forces and moments on an oscillating airfoil for the rotary-wing case are more complex than the fixed wing counterpart. Loewy [Ref. 2] determines these forces and moments for the hovering case where $k = \frac{\omega b}{\Omega r}$, but uses a slightly different approach to the problem by solving the integral downwash equation which leads to an equation for the pressure distribution which is in the same form as Theodorsen. Loewy then defines a modified lift deficiency function, and states that the integration of the pressure distribution across the airfoil would be identical to Theodorsen. This makes the expressions for forces and moments identical except for a modified lift deficiency function.

The first step that Loewy performs is to set up a system to account for the wakes generated by the previous blades in the same revolution and all blades in previous revolutions as shown in Figure 4. He uses two indices to account for the vorticity shed by a given wake: n indicates the revolution and q indicates the blade whose wake it is. The induced velocity or downwash resulting from an element of vorticity is obtained from the Biot-Savart Theorem,

$$dw(x) = \frac{\gamma_{n,q}(x-\xi) d\xi}{2\pi[(x-\xi)^2 + (nQ+q)^2 h^2]} , \quad (37)$$

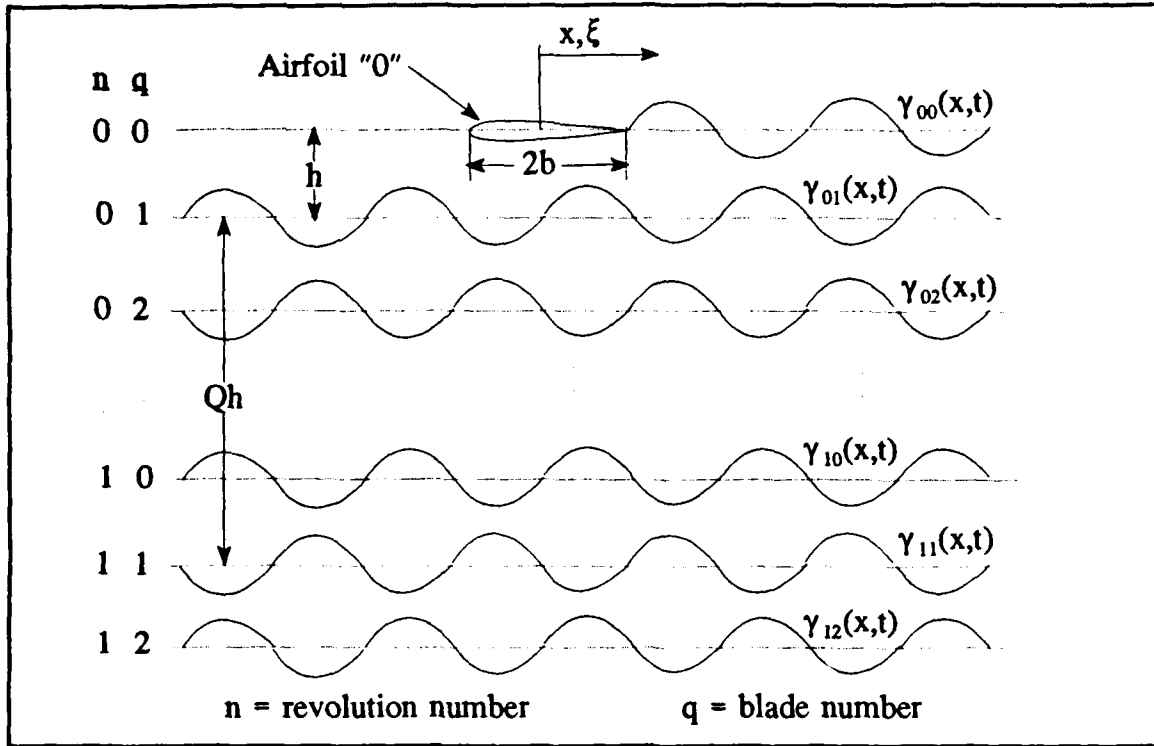


Figure 4. Aerodynamic model for a multi-blade rotor system.

where γ_{nq} is the vorticity, Q is the number of rotor blades, and h is the non-dimensional wake spacing. Writing the integrals involving the bound vorticity and the vorticity in the wake of the reference airfoil separately from the rows of vorticity below the plane of the rotor yield

$$w(x) = -\frac{1}{2\pi} \left[\int_{-1}^1 \frac{\gamma_s(\xi) d\xi}{x-\xi} + \int_1^\infty \frac{\gamma_{00}(\xi) d\xi}{x-\xi} + \sum_{q=1}^{Q-1} \sum_{n=0}^{\infty} \int_{-\infty}^{\infty} \frac{\gamma_{nq}(\xi)(x-\xi) d\xi}{(x-\xi)^2 + (nQ+q)^2 h^2} + \sum_{n=1}^{\infty} \int_{-\infty}^{\infty} \frac{\gamma_{n0}(\xi)(x-\xi) d\xi}{(x-\xi)^2 + n^2 Q^2 h^2} \right] \quad (38)$$

In essence the problem has been broken down in the same manner as Theodorsen. The first integral represents the effects of the freestream on the airfoil (non-circulatory

terms). The second integral represents the velocity created by the vorticity generated by the reference wake (circulatory term). The third and fourth integrals represent the velocity created by the vorticity generated by previous blades or in previous revolutions (circulatory terms). The main difference between Loewy and Theodorsen is the terms which account for the vorticity generated by previous blades or in previous revolutions.

Loewy [Ref. 2] shows that the vorticity shed by the q th blade in the n th revolution is

$$\gamma_{nq} = ik\Gamma e^{[i(\psi_q - k\xi - 2\pi m q/Q - 2\pi mn)]}, \quad (39)$$

where Γ is the total circulation around the airfoil, ψ_q is the phase angle by which the motion of the q th blade leads that of the reference blade, and m is the ratio of oscillatory frequency to rotational frequency. Substituting the vorticity expression from equation (39) into the integral downwash equation (38) yields

$$\begin{aligned} w(x) = & -\frac{1}{2\pi} \left[\int_{-1}^1 \frac{\gamma_s(\xi) d\xi}{x - \xi} - ik\Gamma \int_1^\infty \frac{e^{-ik\xi} d\xi}{x - \xi} \right. \\ & - ik\Gamma \sum_{q=1}^{Q-1} e^{-i(2\pi m q/Q - \psi_q)} \sum_{n=0}^\infty e^{-i2\pi mn} \int_{-\infty}^\infty \frac{e^{-ik\xi} (x - \xi) d\xi}{(x - \xi)^2 + (nQ + q)^2 h^2} \\ & \left. - ik\Gamma \sum_{n=1}^\infty e^{-i2\pi mn} \int_{-\infty}^\infty \frac{e^{-ik\xi} (x - \xi) d\xi}{(x - \xi)^2 + n^2 Q^2 h^2} \right]. \end{aligned} \quad (40)$$

The last two integrals in equation (40) have the form

$$\int_{-\infty}^\infty \frac{e^{-ik\xi} (x - \xi) d\xi}{(x - \xi)^2 + A^2} = i\pi e^{-k(ix + A)}. \quad (41)$$

Substituting equation (41) into equation (40) and noting that the summations over n are convergent geometric series give

$$w(x) = -\frac{1}{2\pi} \left[\int_{-1}^1 \frac{\gamma_s(\xi) d\xi}{(x-\xi)} - ik\Gamma \int_1^\infty \frac{e^{-ik\xi} d\xi}{(x-\xi)} + \pi k\Gamma e^{-ikx} W(k, h, m) \right], \quad (42)$$

where

$$W(k, h, m) = \frac{1 + \sum_{q=1}^{Q-1} (e^{khQ} e^{i2\pi m})^{(Q-q)/Q} e^{i\psi_q}}{e^{khQ} e^{i2\pi m} - 1}. \quad (43)$$

The function $W(k, h, m)$ may be thought of as a weighting function for the vorticity shed by previous blades or in previous revolutions.

The form of the downwash equation in equation (42) can be solved by applying Söhngen's inversion formula [Ref. 14], which shows that the solution to an equation in the form

$$g(x) = \frac{1}{2\pi} \int_{-1}^1 \frac{f(\xi) d\xi}{x-\xi} \quad (44)$$

is

$$f(x) = -\frac{2}{\pi} \sqrt{\frac{1-x}{1+x}} \int_{-1}^1 \sqrt{\frac{1+\xi}{1-\xi}} \frac{g(\xi) d\xi}{x-\xi}. \quad (45)$$

Satisfying the condition $f(1) = \text{finite}$ is the same as employing the Kutta condition.

The bound vorticity becomes

$$\begin{aligned} \gamma_s(x) = & \frac{2}{\pi} \sqrt{\frac{1-x}{1+x}} \left[\int_{-1}^1 \sqrt{\frac{1+\xi}{1-\xi}} \frac{w(\xi) d\xi}{x-\xi} \right. \\ & - \frac{ik\Gamma}{2\pi} \int_{-1}^1 \sqrt{\frac{1+\xi}{1-\xi}} \left(\frac{1}{x-\xi} \right) \int_1^\infty \frac{e^{-ik\eta} d\eta}{\xi-\eta} d\xi \\ & \left. + \frac{k\Gamma}{2} W(k,h,m) \int_{-1}^1 \sqrt{\frac{1+\xi}{1-\xi}} \frac{e^{-ik\xi} d\xi}{x-\xi} \right]. \end{aligned} \quad (46)$$

Evaluating the circulation over the entire airfoil yields

$$\Gamma = e^{ik} \int_{-1}^1 \gamma_s(x) dx = \frac{2 \int_{-1}^1 \sqrt{\frac{1+\xi}{1-\xi}} w(\xi) d\xi}{i\pi k \left[\frac{1}{2} (H_1^{(2)} + iH_0^{(2)}) + (J_1 + iJ_0) W(k,h,m) \right]}, \quad (47)$$

where the Hankel and Bessel functions are evaluated at reduced frequency (k).

Since the airfoil can be thought of as a vortex sheet, the generalized Bernoulli equation (4) becomes

$$\Delta p(x) = -\rho \left[v \gamma_s(x,t) + b \frac{\partial}{\partial t} \int_{-1}^x \gamma_s(\xi,t) d\xi \right]. \quad (48)$$

If simple harmonic motion is assumed,

$$\frac{\partial}{\partial t} \gamma_s = i\omega \gamma_s, \quad (49)$$

and equation (48) becomes

$$\Delta p(x) = -\rho \left[v \gamma_s(x,t) + i\omega b \int_{-1}^x \gamma_s(\xi,t) d\xi \right]. \quad (50)$$

Substituting the bound vorticity equation (46) and the airfoil circulation equation (47) into equation (50) yield

$$\begin{aligned}
-\frac{\Delta p(x)}{\rho \Omega r} = & \frac{\frac{2i}{\pi} [H_0^{(2)} + 2J_0 W(k, h, m)]}{H_1^{(2)} + iH_0^{(2)} + 2[J_1 + iJ_0] W(k, h, m)} \int_{-1}^1 \sqrt{\frac{1-x}{1+x}} \sqrt{\frac{1+\xi}{1-\xi}} w(\xi) d\xi \\
& + \frac{2}{\pi} \int_{-1}^1 \left[\sqrt{\frac{1-x}{1+x}} \sqrt{\frac{1+\xi}{1-\xi}} \left(\frac{1}{x-\xi} \right) \right. \\
& \quad \left. - \frac{ik}{2} \log \left(\frac{1-x\xi - \sqrt{1-x^2}\sqrt{1-\xi^2}}{1-x\xi + \sqrt{1-x^2}\sqrt{1-\xi^2}} \right) \right] w(\xi) d\xi .
\end{aligned} \tag{51}$$

The pressure distribution in equation (51) has the same form as Theodorsen's in equation (17) if the factor multiplying the first integral is written as

$$\frac{2}{\pi} [1 - C'(k, h, m)] , \tag{52}$$

where $C'(k, h, m)$ is Loewy's lift deficiency function. Solving for $C'(k, h, m)$ yields

$$C'(k, h, m) = \frac{H_1^{(2)} + 2J_1 W(k, h, m)}{H_1^{(2)} + iH_0^{(2)} + 2[J_1 + iJ_0] W(k, h, m)} , \tag{53}$$

where the Hankel and Bessel functions are evaluated at reduced frequency (k). Since $C'(k, h, m)$ is not a function of location along the airfoil, the integration of the pressure distribution in equation (51) across the airfoil will yield equations of motion identical to Theodorsen's in equations (18) and (19) except $C(k)$ will be replaced by $C'(k, h, m)$. It can be seen that as $W(k, h, m)$ approaches zero, $C'(k, h, m) = C(k)$, and this condition corresponds to an infinite wake spacing ($h \rightarrow \infty$).

Since the wake weighting function is periodic in nature, Loewy [Ref. 2] shows that the wake weighting function for a multi-blade rotor can be expressed by a single-blade

rotor with modified values of h and m will yield the same value of W . For a single-blade rotor, the wake weighting function becomes

$$W(k, h, m) = \frac{1}{e^{kh} e^{i2\pi m} - 1}, \quad (54)$$

where h and m are the modified values of wake spacing and frequency ratio respectively. For the case of the single-blade rotor the wake weighting function can be separated into its real and imaginary parts,

$$W(k, h, m) = \hat{\alpha} + i\hat{\beta}, \quad (55)$$

where

$$\hat{\alpha} = \frac{\cos 2\pi m - e^{-kh}}{e^{kh} - 2\cos 2\pi m + e^{-kh}} \quad (56)$$

and

$$\hat{\beta} = \frac{-\sin 2\pi m}{e^{kh} - 2\cos 2\pi m + e^{-kh}}. \quad (57)$$

Separating Loewy's lift deficiency function into its real and imaginary parts similar to Theodorsen yields⁴

$$C'(k, h, m) = F' + iG' \quad (58)$$

where

⁴This is equivalent to Loewy's equations in reference 2 when the substitutions $\alpha = 1 + 2\hat{\alpha}$ and $\beta = -2\hat{\beta}$ are used.

$$F' = \frac{J_1(1+2\hat{\alpha})A - (Y_1 - 2J_1\hat{\beta})B}{A^2 + B^2} \quad (59)$$

$$G' = -\frac{(Y_1 - 2J_1\hat{\beta})A + J_1(1+2\hat{\alpha})B}{A^2 + B^2} \quad (60)$$

and

$$A = J_1(1+2\hat{\alpha}) + Y_0 - 2J_0\hat{\beta} \quad (61)$$

$$B = -Y_1 + 2J_1\hat{\beta} + J_0(1+2\hat{\alpha}) . \quad (62)$$

Plots of Loewy's lift deficiency function are shown in Figures 5 through 8. It is easily seen that there are rapid changes in the lift deficiency function as reduced frequency (k), wake spacing (h), and frequency (m) vary.

Since Loewy's lift deficiency function is completely analogous to Theodorsen's lift deficiency function, the propulsive force determined by Garrick [Ref. 3] and the propulsive force coefficient can be calculated for the rotary-wing case by substituting F' and G' for F and G . For pure plunge ($\alpha_o = 0$)

$$C_{P_x} = \pi k^2 \bar{h}_o^2 \left((F')^2 + (G')^2 \right) , \quad (63)$$

for pure pitch ($h_o = 0$)

$$C_{P_x} = \pi k^2 \alpha_o^2 \left\{ \left((F')^2 + (G')^2 \right) \left[\frac{1}{k^2} + \left(\frac{1}{2} - a \right)^2 \right] + \frac{1}{2} \left(\frac{1}{2} - a \right) - (F') \left(\frac{1}{2} - a + \frac{1}{k^2} \right) - \left(\frac{1}{2} + a \right) \frac{(G')}{k} \right\} , \quad (64)$$

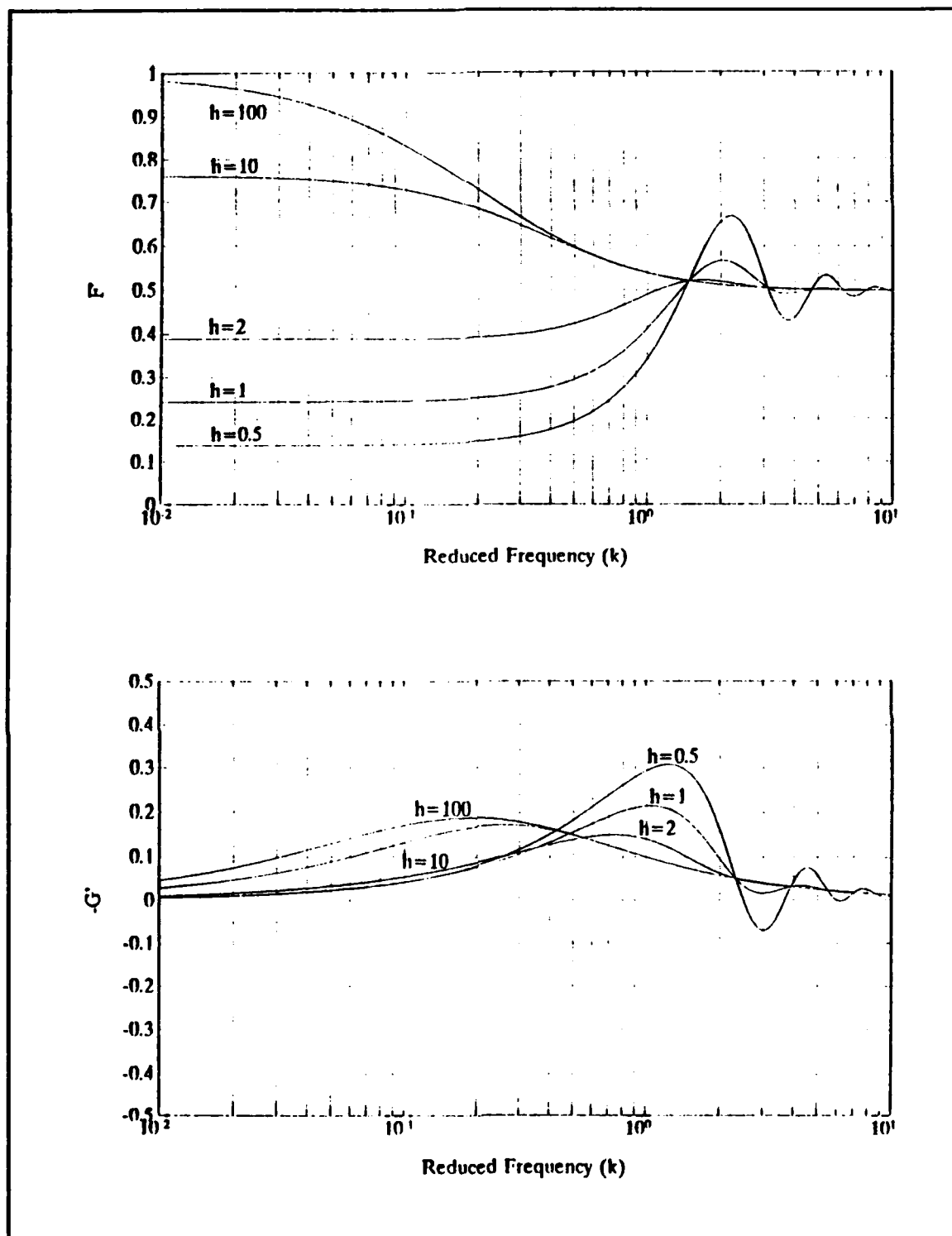


Figure 5. Loewy's lift deficiency function as a function of wake spacing for $m = 0$.

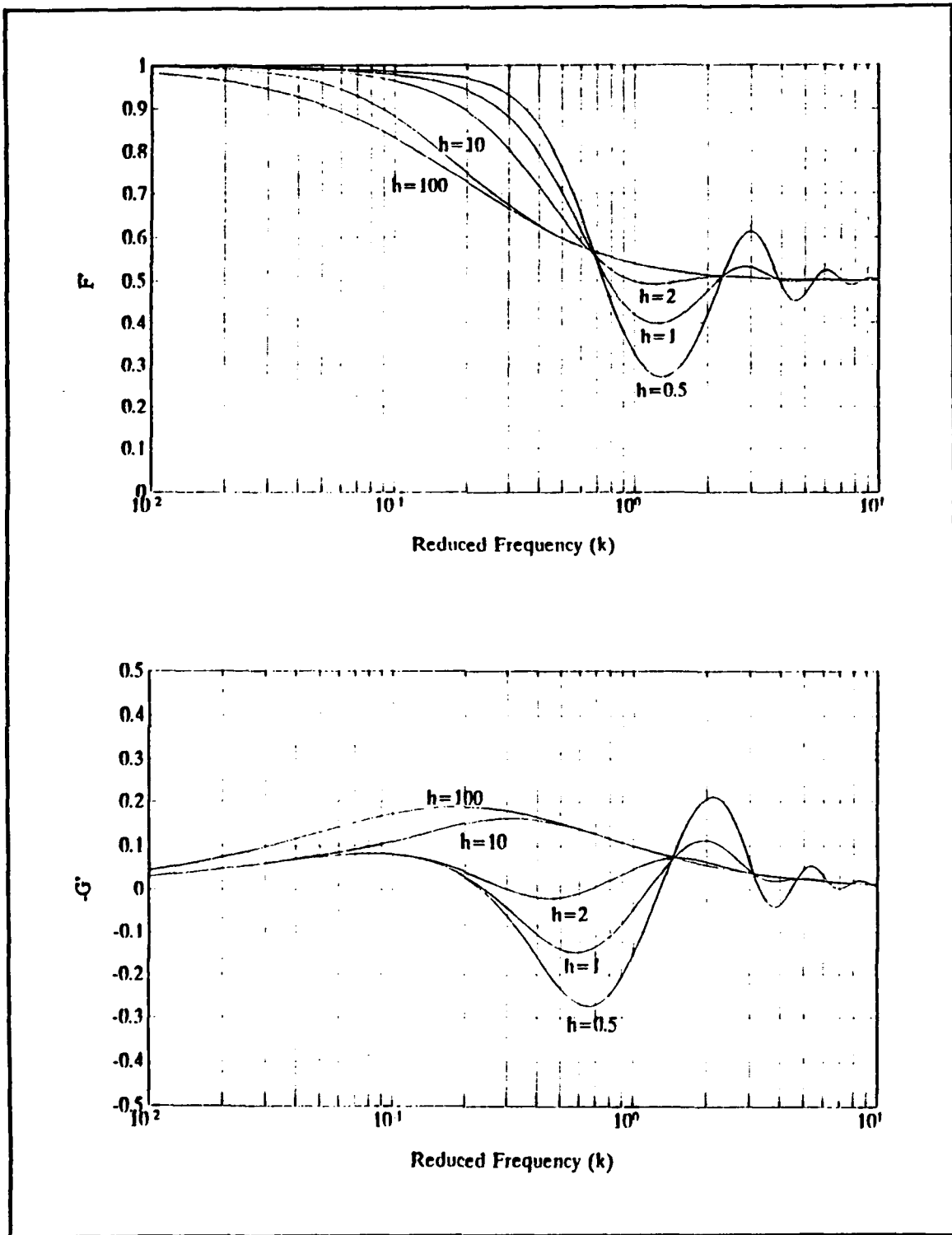


Figure 6. Loewy's lift deficiency function as a function of wake spacing for $m = 0.25$.

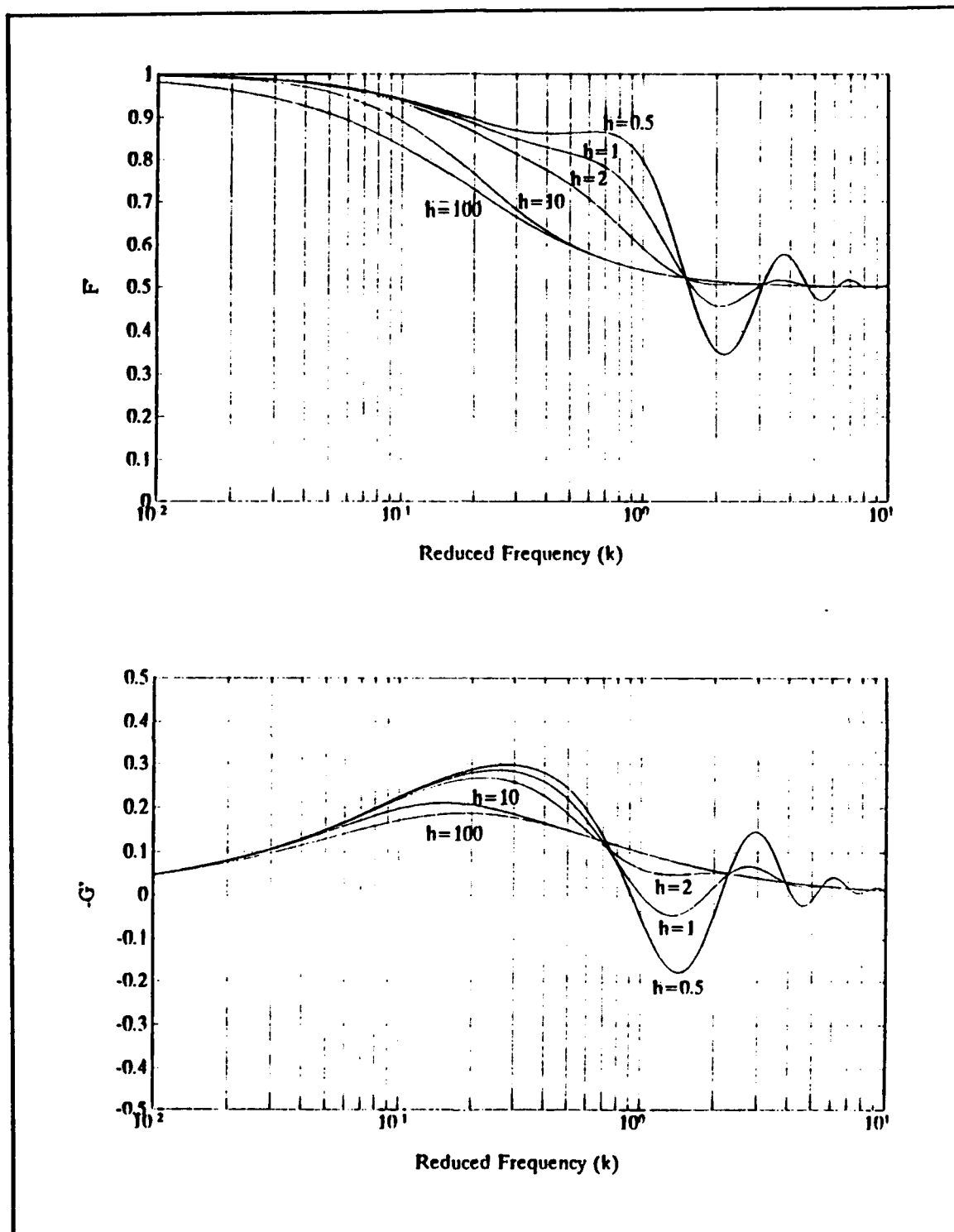


Figure 7. Loewy's lift deficiency function as a function of wake spacing for $m = 0.5$.

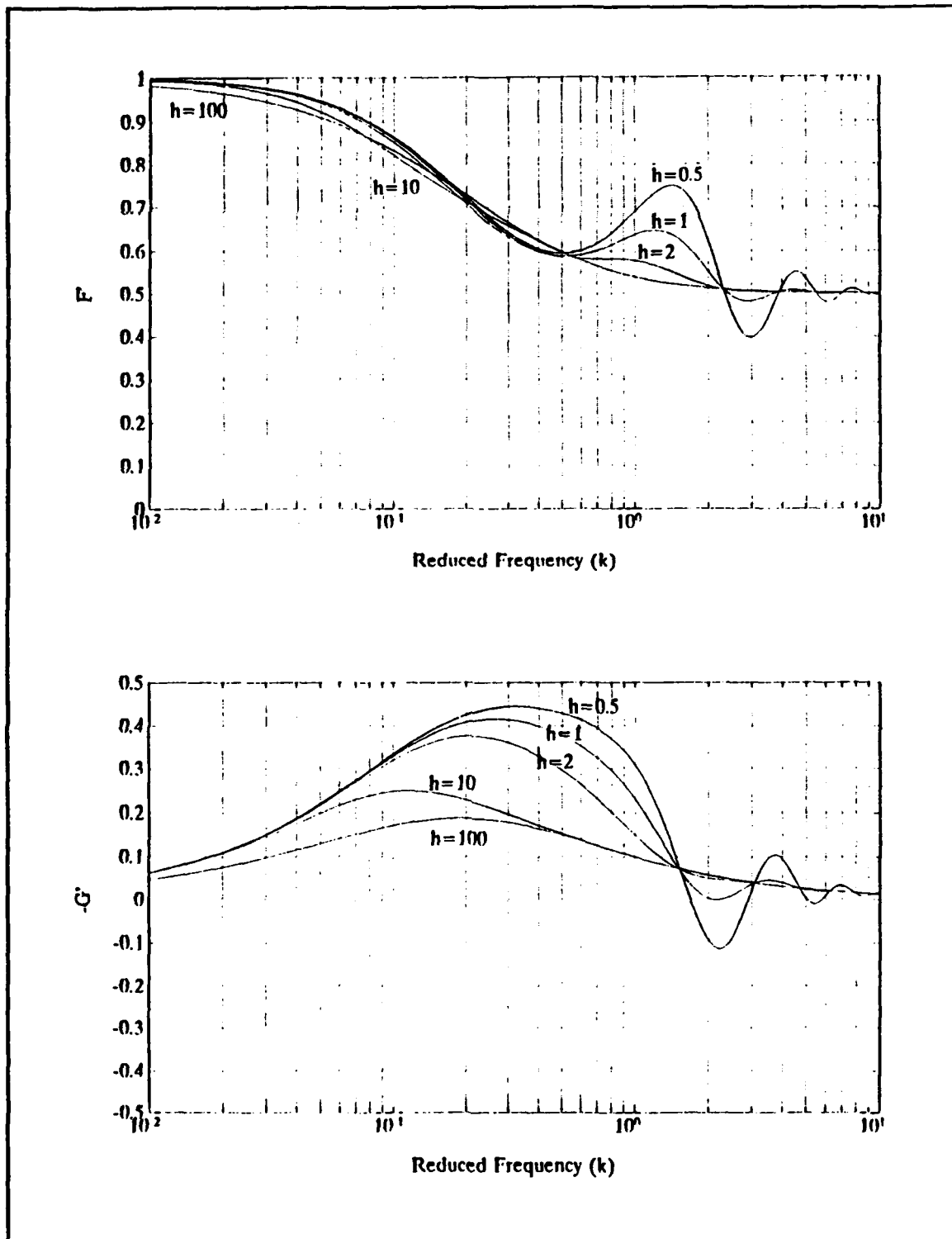


Figure 8. Loewy's lift deficiency function as a function of wake spacing for $m = 0.75$.

and for coupled pitch and plunge

$$\begin{aligned}
 C_{P_x} = \pi k^2 \bigg\{ & \bar{h}_o^2 \left[(F')^2 + (G')^2 \right] \\
 & + \alpha_o^2 \left[\left((F')^2 + (G')^2 \right) \left(\frac{1}{k^2} + \left(\frac{1}{2} - a \right)^2 \right) \right. \\
 & \quad \left. + \frac{1}{2} \left(\frac{1}{2} - a \right) \left((F') \left(\frac{1}{2} - a + \frac{1}{k^2} \right) - \left(\frac{1}{2} + a \right) \frac{(G')}{k} \right) \right] \\
 & \left. + \alpha_o \bar{h}_o \left[\left(\frac{1}{2} - a \right) \left((F')^2 + (G')^2 \right) + \frac{1}{2} \left(\frac{1}{2} - \frac{(G')}{k} - (F') \right) \right] \right\} .
 \end{aligned} \tag{65}$$

Plots of propulsive force coefficient as a function of frequency ratio for $k = 0.1234$ are shown in Figure 9 through 11. It can be seen that C_{P_x} is reasonably constant for $0.15 < m < 0.8$ and greater than the "Katzmayr effect." (In this case $h = 100$ is sufficient to represent $h \rightarrow \infty$). For $m < 0.15$ and $m > 0.8$, C_{P_x} begins to decrease to the point where it eventually becomes less than the "Katzmayr effect."

B. FINITE WAKE LIFT DEFICIENCY FUNCTION

1. General

Loewy's theory can be extended to the case of a finite number of wakes below the rotor blade by modifying the wake weighting function. This modified wake weighting function is completely analogous with Loewy's which makes the definition of the lift deficiency function the same, but with $\hat{\alpha}$ and $\hat{\beta}$ modified by the new wake weighting function. Since the lift deficiency function is of the same form, the aerodynamic forces and moments will be the same, but with a modified lift deficiency function. Loewy has already shown that the rotary-wing problem reduces to the case of a single rotor. The modified wake weighting function will also be developed for

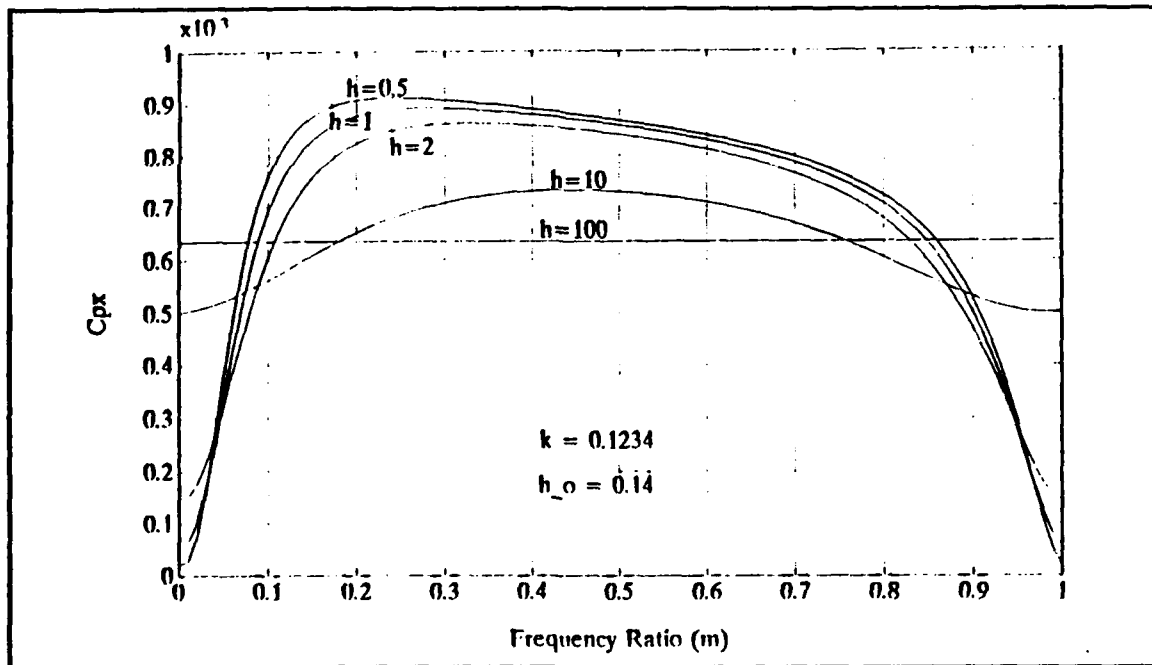


Figure 9. Propulsive force coefficient in pure plunge as a function of wake spacing with an infinite number of wakes (Loewy's lift deficiency function).

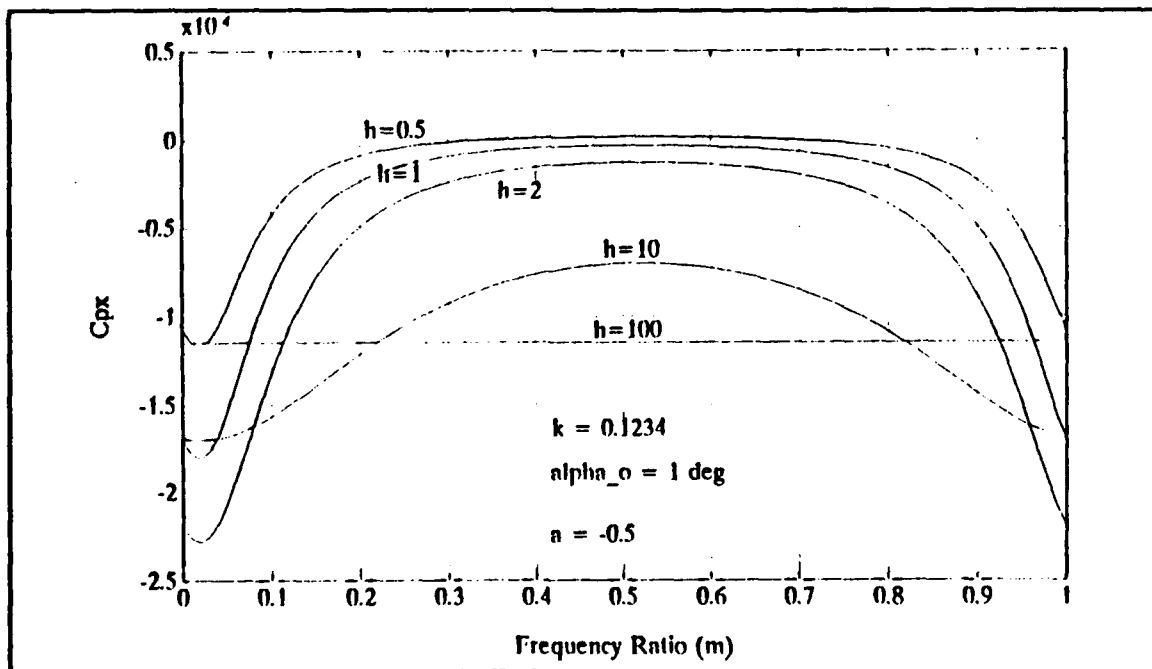


Figure 10. Propulsive force coefficient in pure pitch as a function of wake spacing with an infinite number of wakes (Loewy's lift deficiency function).

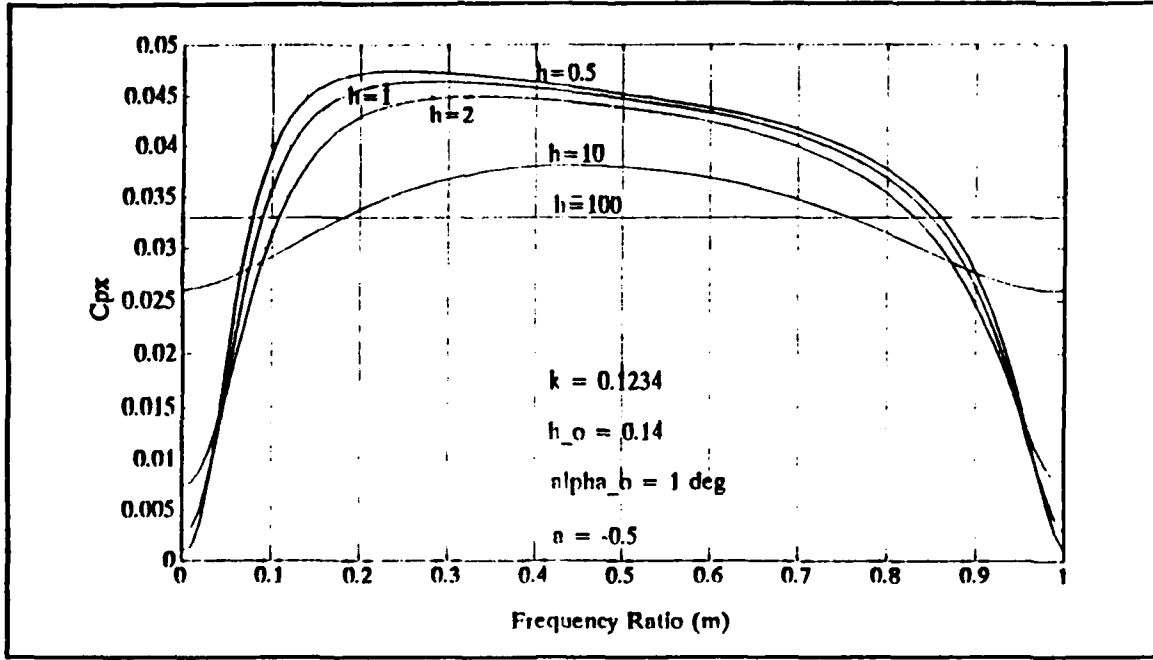


Figure 11. Propulsive force coefficient in coupled pitch-plunge as a function of wake spacing with an infinite number of wakes (Loewy's lift deficiency function).

the case of the multi-blade rotor, and then reduced to the case of the single-blade rotor with modified wake spacing and frequency ratio.

The development of a finite wake lift deficiency function is the same as Loewy's described earlier. Changing the integral downwash equation (40) to a finite number (N) of revolutions yields

$$\begin{aligned}
 w(x) = & -\frac{1}{2\pi} \left[\int_{-1}^1 \frac{\gamma_s(\xi) d\xi}{x-\xi} - ik\Gamma \int_1^\infty \frac{e^{-ik\xi} d\xi}{x-\xi} \right. \\
 & - ik\Gamma \sum_{q=1}^{Q-1} e^{-i(2\pi m q/Q - \psi_q)} \sum_{n=0}^N e^{-i2\pi m n} \int_{-\infty}^\infty \frac{e^{-ik\xi} (x-\xi) d\xi}{(x-\xi)^2 + (nQ+q)^2 h^2} \\
 & \left. - ik\Gamma \sum_{n=1}^N e^{-i2\pi m n} \int_{-\infty}^\infty \frac{e^{-ik\xi} (x-\xi) d\xi}{(x-\xi)^2 + n^2 Q^2 h^2} \right], \quad (66)
 \end{aligned}$$

where the summations from n equal zero to infinity have been replaced by finite summations from n equal zero to N . Using equation (41) to solve the last two integrals in equation (66) results in

$$w(x) = -\frac{1}{2\pi} \left[\int_{-1}^1 \frac{\gamma_s(\xi) d\xi}{x-\xi} - ik\Gamma \int_1^\infty \frac{e^{-ik\xi} d\xi}{x-\xi} + \pi k\Gamma e^{-ikx} \left(\sum_{q=1}^{Q-1} e^{-i(2\pi m q/Q - \psi_q)} \sum_{n=0}^N e^{-i2\pi mn} e^{-k(nQ+q)h} + \sum_{n=1}^N e^{-i2\pi mn} e^{-nQkh} \right) \right]. \quad (67)$$

Since this is in the same form as equation (42), the terms enclosed by the parentheses can be defined as the finite wake weighting function, or

$$W_N(k, h, m) = \sum_{q=1}^{Q-1} e^{-i(2\pi m q/Q - \psi_q)} \sum_{n=0}^N e^{-i2\pi mn} e^{-k(nQ+q)h} + \sum_{n=1}^N e^{-i2\pi mn} e^{-nQkh}. \quad (68)$$

It is easily seen that this modified wake weighting function is periodic once the relationship ψ_q is known, and a multi-blade rotor can be reduced to a single-blade rotor with modified wake spacing and frequency ratio. For the case of the single-blade rotor ($Q = 1$),

$$W_N(k, h, m) = \sum_{n=1}^N e^{-i2\pi mn} e^{-nkh}. \quad (69)$$

It can be shown that as $N \rightarrow \infty$, the finite wake weighting function in equation (69) becomes a convergent geometric series equivalent to Loewy's wake weighting function in equation (54) provided $m \neq 0$ and $h \neq 0$. A singularity in the solution exists when $m = 0$ and $h = 0$, and the case of $h = 0$ has no real physical significance.

The solution to the remainder of the finite wake problem is identical to Loewy, but using the modified finite wake lift deficiency function. To keep the finite wake lift deficiency function separate from Loewy's lift deficiency function, the former is defined as follows:

$$C^*(k, h, m) = \frac{H_1^{(2)} + 2 J_1 W_N}{H_1^{(2)} + i H_0^{(2)} + 2 [J_1 + i J_0] W_N} . \quad (70)$$

Separating the finite wake weighting function in equation (69) into real and imaginary parts,

$$W_N = \hat{\alpha}_N + i \hat{\beta}_N , \quad (71)$$

yields

$$\hat{\alpha}_N = \sum_{n=1}^N e^{-nkh} \cos 2\pi mn \quad (72)$$

and

$$\hat{\beta}_N = \sum_{n=1}^N (-e^{-nkh} \sin 2\pi mn) . \quad (73)$$

The finite wake lift deficiency function becomes

$$C^* = F^* + i G^* , \quad (74)$$

where

$$F^* = \frac{J_1(1+2\hat{\alpha}_N)A_N - (Y_1 - 2J_1\hat{\beta}_N)B_N}{A_N^2 + B_N^2} \quad (75)$$

$$G^* = -\frac{(Y_1 - 2J_1\hat{\beta}_N)A_N + J_1(1+2\hat{\alpha}_N)B_N}{A_N^2 + B_N^2} \quad (76)$$

and

$$A_N = J_1(1+2\hat{\alpha}_N) + Y_0 - 2J_0\hat{\beta}_N \quad (77)$$

$$B_N = -Y_1 + 2J_1\hat{\beta}_N + J_0(1+2\hat{\alpha}_N) . \quad (78)$$

2. Single Wake Case

For the case of a single wake, the wake weighting function reduces to

$$W_1 = e^{-(i2\pi m + kh)} , \quad (79)$$

where

$$\hat{\alpha}_1 = e^{-kh} \cos 2\pi m \quad (80)$$

and

$$\hat{\beta}_1 = -e^{-kh} \sin 2\pi m . \quad (81)$$

Plots of the single wake lift deficiency function are shown in Figures 12 through 15.

The propulsive force coefficient can be calculated by replacing F and G in equations (34), (35), and (36) with F^* and G^* . For pure plunge ($\alpha_o = 0$)

$$C_{P_i} = \pi k^2 \bar{h}_o^2 \left\{ (F^*)^2 + (G^*)^2 \right\}, \quad (82)$$

for pure pitch ($h_o = 0$)

$$C_{P_i} = \pi k^2 \alpha_o^2 \left\{ \left[(F^*)^2 + (G^*)^2 \right] \left[\frac{1}{k} + \left(\frac{1}{2} - a \right)^2 \right] + \frac{1}{2} \left(\frac{1}{2} - a \right) \right. \\ \left. - (F^*) \left(\frac{1}{2} - a + \frac{1}{k^2} \right) - \left(\frac{1}{2} + a \right) \frac{(G^*)}{k} \right\}, \quad (83)$$

and for coupled pitch and plunge

$$C_{P_i} = \pi k^2 \left\{ \bar{h}_o^2 \left[(F^*)^2 + (G^*)^2 \right] \right. \\ \left. + \alpha_o^2 \left[\left[(F^*)^2 + (G^*)^2 \right] \left[\frac{1}{k^2} + \left(\frac{1}{2} - a \right)^2 \right] \right. \right. \\ \left. \left. + \frac{1}{2} \left(\frac{1}{2} - a \right) - (F^*) \left(\frac{1}{2} - a + \frac{1}{k^2} \right) - \left(\frac{1}{2} + a \right) \frac{(G^*)}{k} \right] \right. \\ \left. + \alpha_o \bar{h}_o \left[\left(\frac{1}{2} - a \right) \left[(F^*)^2 + (G^*)^2 \right] + \frac{1}{2} \left(\frac{1}{2} - \frac{(G^*)}{k} - (F^*) \right) \right] \right\}. \quad (84)$$

Plots of the propulsive force coefficient as a function of frequency ratio for $k = 0.1234$ are shown in Figures 16 through 18. It is interesting to note that for $0.24 < m < 0.7$ the propulsive force is greater than the "Katzmayr effect" with the maximum occurring just prior to $m = 0.5$. Comparing Figures 9, 10, and 11 with Figures 16, 17, and 18

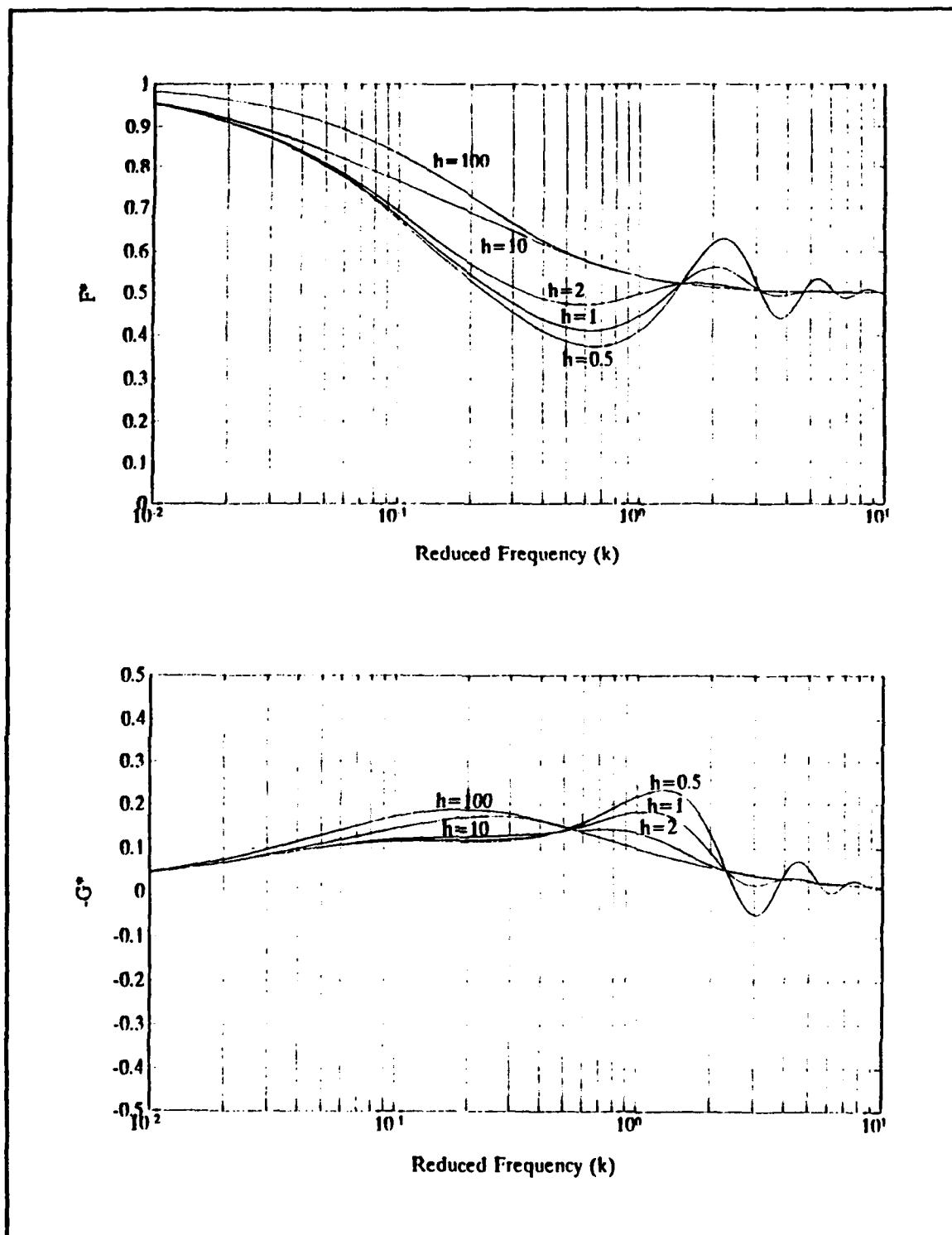


Figure 12. Single wake lift deficiency function as a function of wake spacing for $m = 0$.

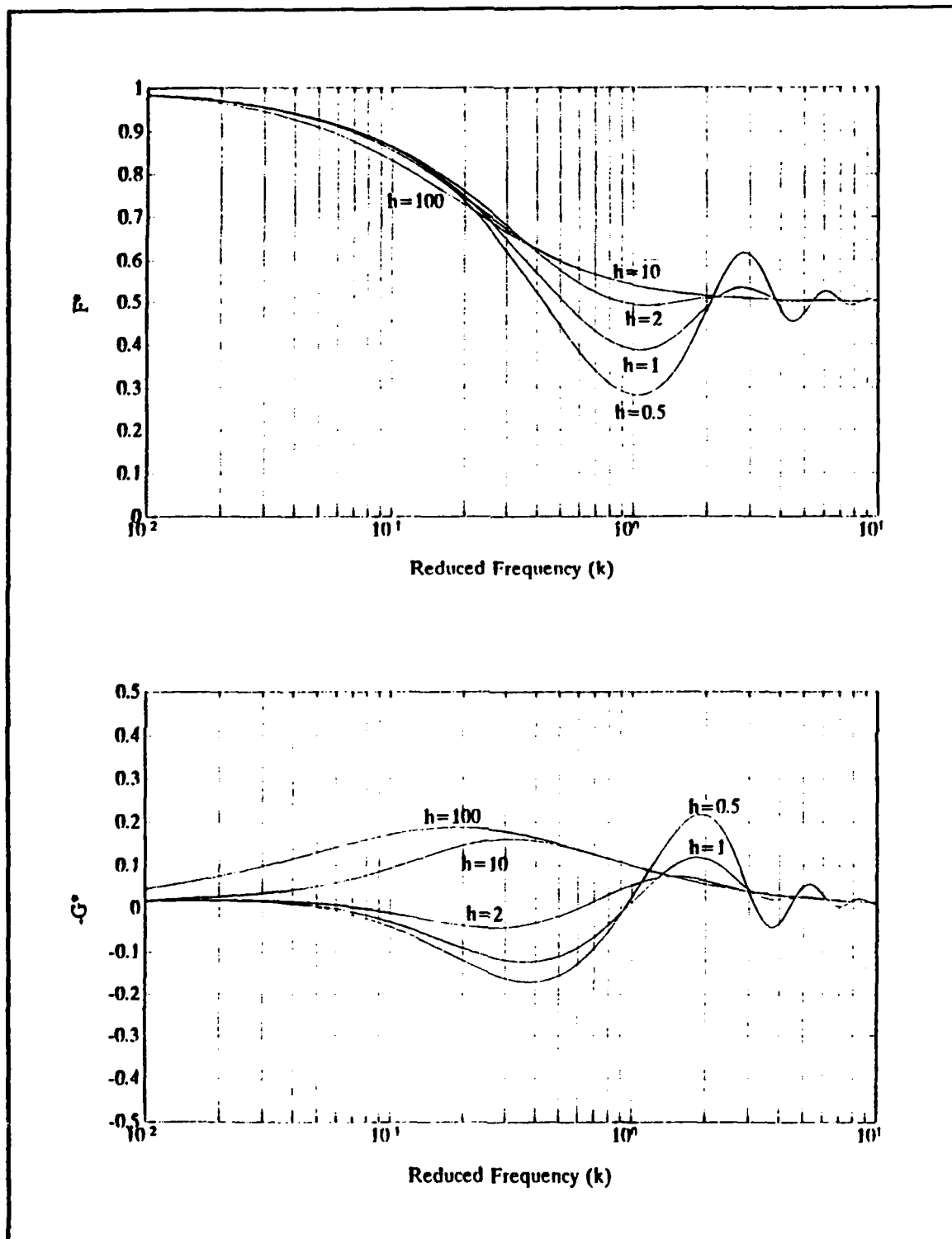


Figure 13. Single wake lift deficiency function as a function of wake spacing for $m = 0.25$.

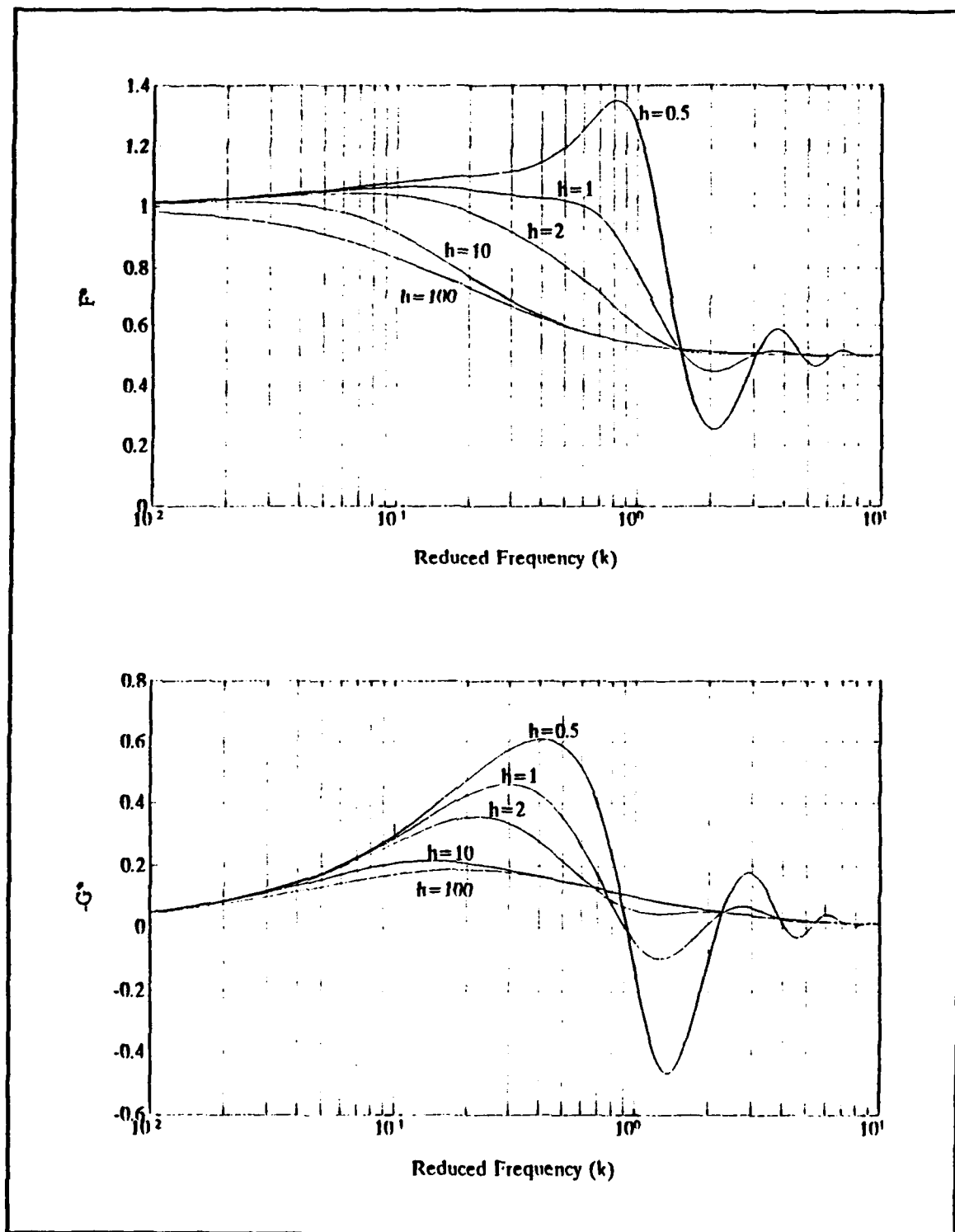


Figure 14. Single wake lift deficiency function as a function of wake spacing for $m = 0.5$.

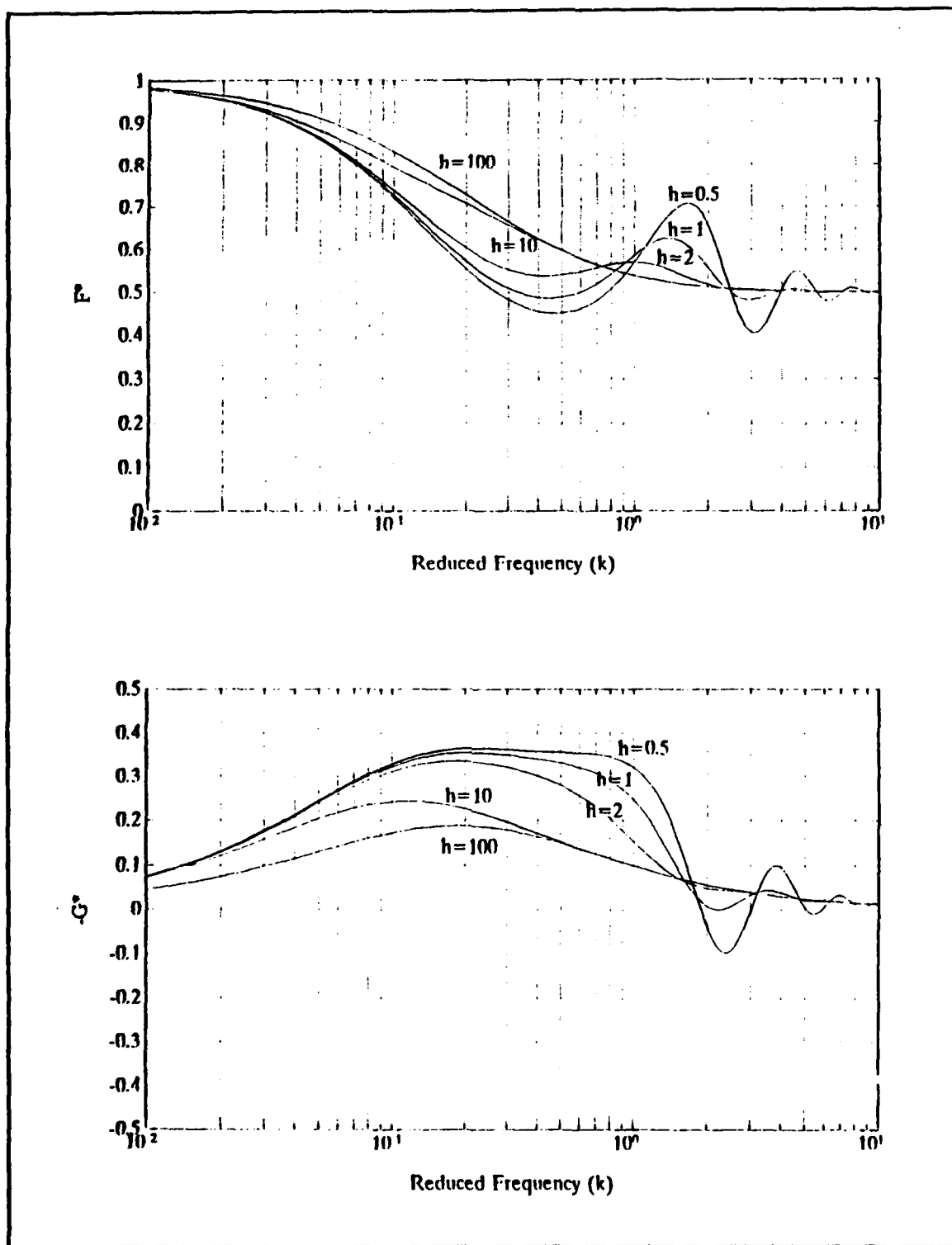


Figure 15. Single wake lift deficiency function as a function of wake spacing for $m = 0.75$.

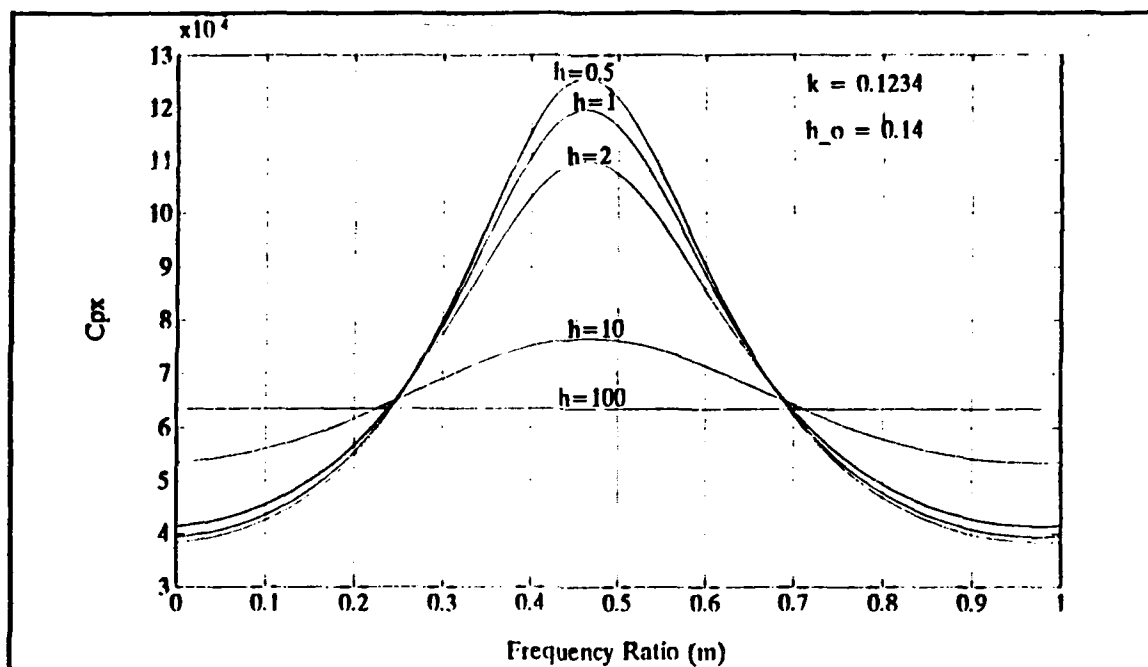


Figure 16. Propulsive force coefficient in pure plunge as a function of wake spacing with a single wake.

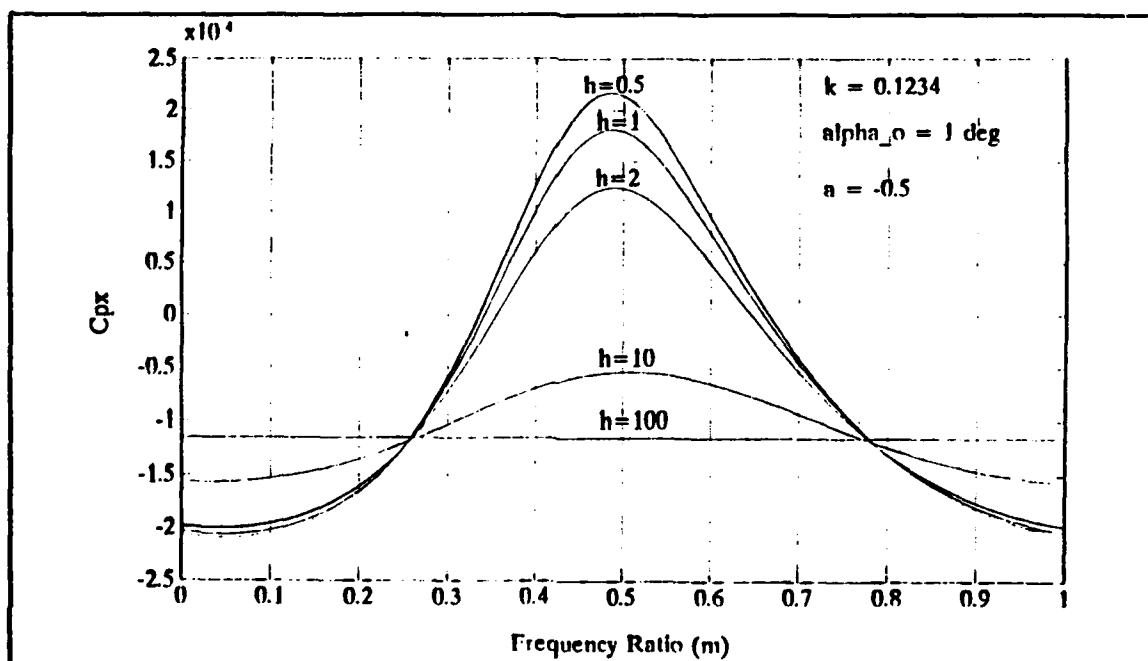


Figure 17. Propulsive force coefficient in pure pitch as a function of wake spacing with a single wake.

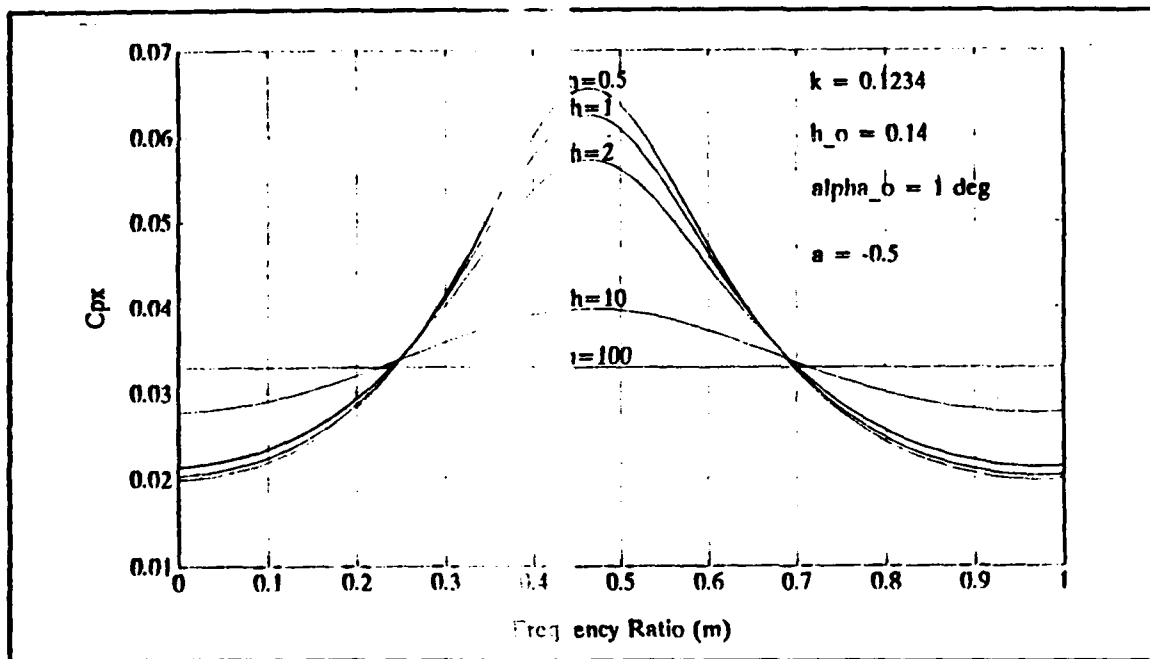


Figure 18. Propulsive force coefficient in coupled pitch-plunge as a function of wake spacing with a single wake.

respectively, the maximum propulsive force (at approximately $m = 0.5$) for a single wake is always greater than the infinite number of wakes. The reason for this increase is that the absolute value of C and C' are never greater than 1.0, but C' as m approaches 0.5 exceeds 1.0 for certain wake spacings.

When $m = 0.5$, this corresponds to the wakes being 180° out of phase as shown in Figure 19, and the vortex from the wake of the reference blade in the current revolution is directly above an oppositely spinning vortex from the single wake of the previous blade or revolution. This efficient use of the vortices in the wake causes C' to exceed 1.0. As the number of wakes increases the vortices from lower wakes are not always 180° out of phase with the reference blade. When $m = 0.5$, each wake is 180° out of phase with the wake above and below it. Thus, each wake is in phase

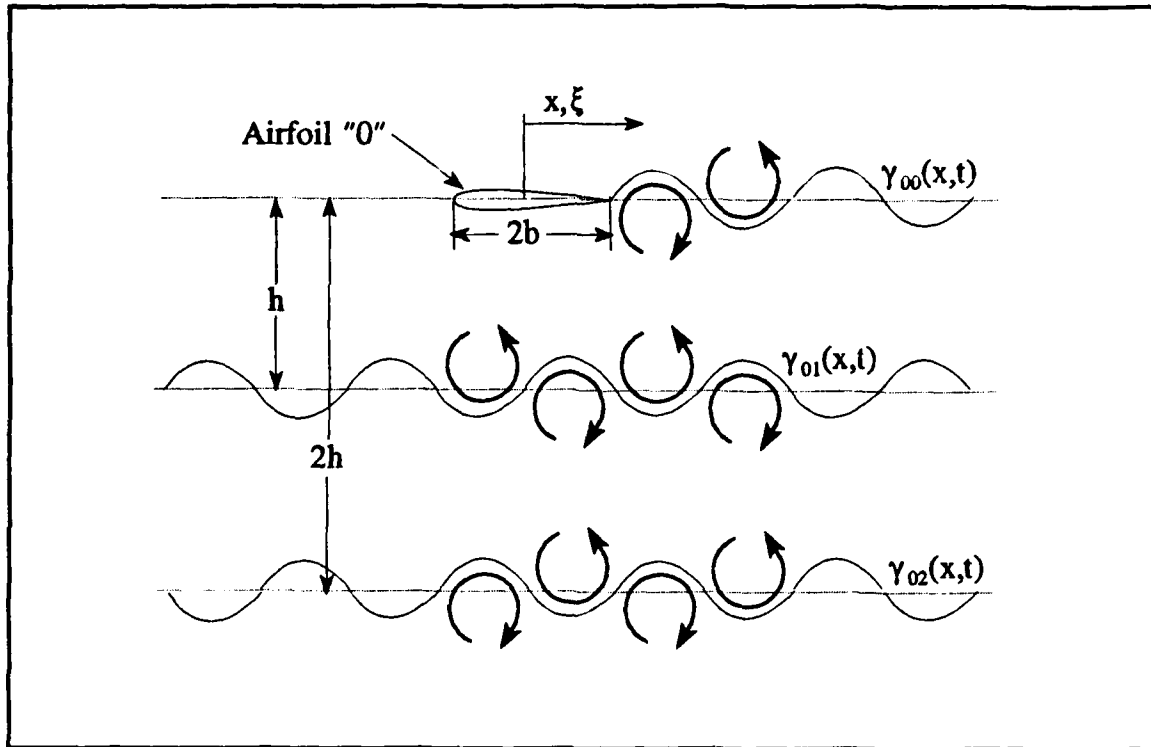


Figure 19. Vortex interaction when wakes are 180° out of phase ($m = 0.5$).

with the wakes ± 2 wake spacings from it. Since the finite wake weighting function contains the term $e^{-i2\pi m}$, the value of each term in the wake weighting function will alternate in sign. However, since the wake spacing is greater for each subsequent wake, the absolute value of each term is not as large as the first term, and thus, the effect of the in-phase wakes are not as strong. As the wake spacing increases this effect diminishes.

3. Multiple Wake Case

When the number of wakes increases, the value of frequency ratio at which the maximum propulsive force coefficient occurs changes as shown in Figures 20 through 22 for $h = 2.0$. This change is analogous to the estimation of a square wave

by a finite number of terms in a Fourier series, where the propulsive force coefficient determined using Loewy's wake weighting function is considered the square wave. As Figures 16 through 18 and 20 through 22 show, an increase in either wake spacing (h) or the number of wakes (N) will decrease the maximum propulsive force that can be obtained. The limit of this decrease will be Loewy's case for a hover.

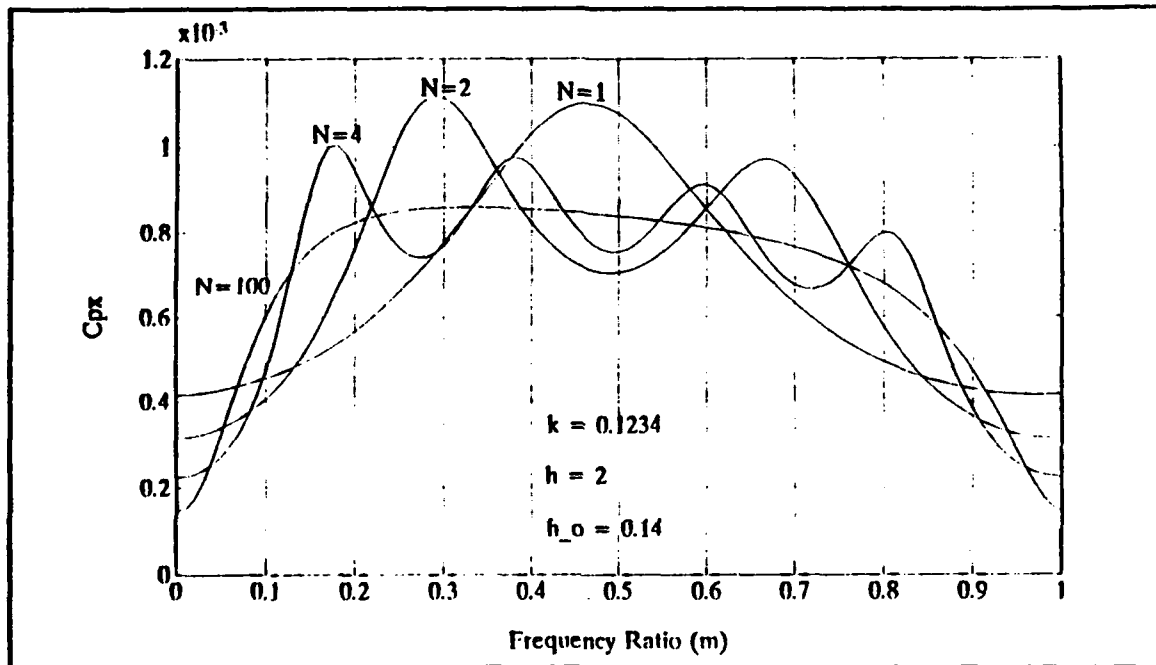


Figure 20. Propulsive force coefficient in pure plunge as a function of the number of wakes at $h = 2.0$.

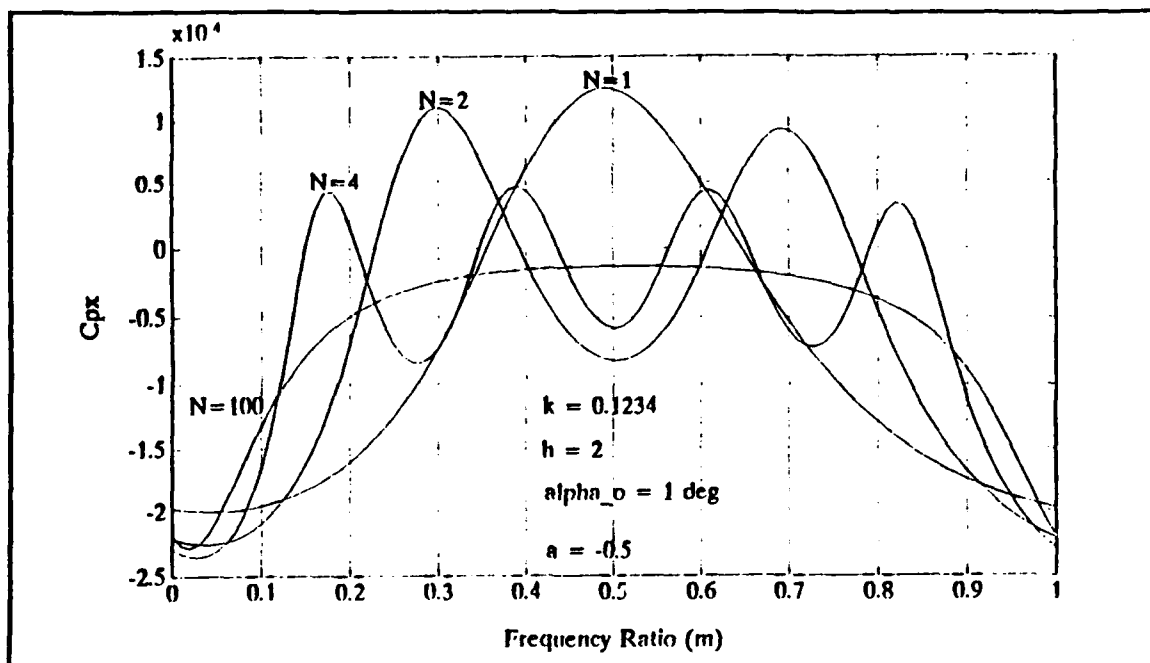


Figure 21. Propulsive force coefficient in pure pitch as a function of the number of wakes at $h = 2.0$.

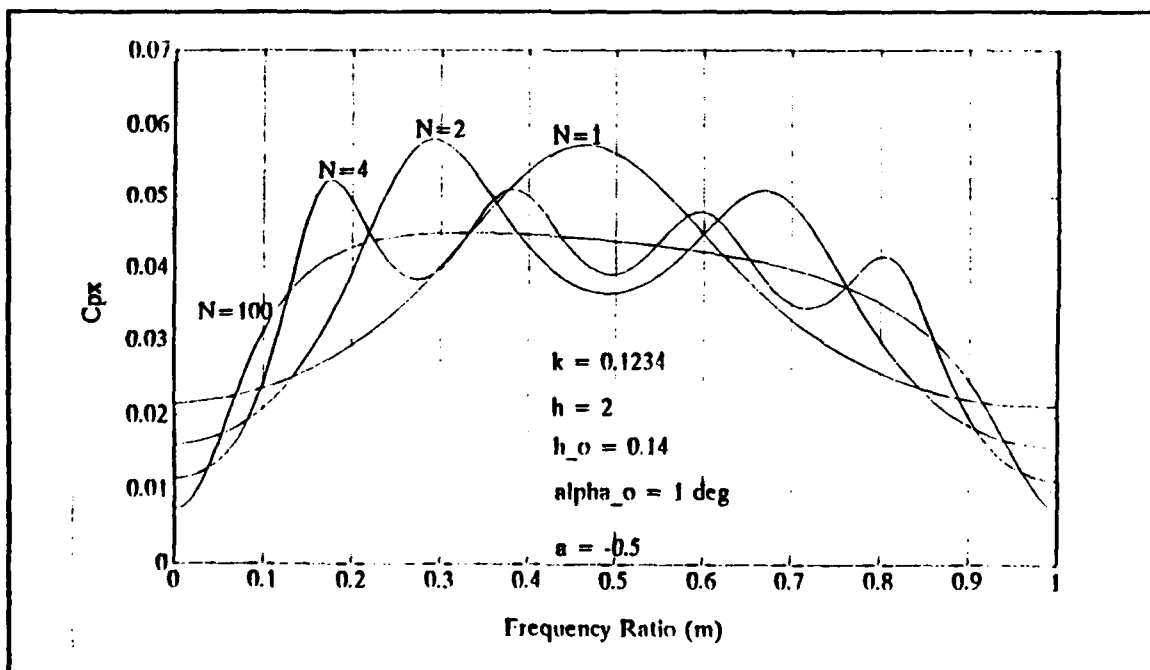


Figure 22. Propulsive force coefficient in coupled pitch-plunge as a function of the number of wakes at $h = 2.0$.

IV. APPLICATIONS

A. EXTENSIONS AND COMPARISON OF THEORY

1. Forward Airspeed

Extension of the finite wake theory can easily be made to include forward airspeed. Shipman and Wood [Ref. 4] expand on Loewy's work incorporating forward airspeed via the advance ratio (μ) into the rotary wing unsteady aerodynamic problem. The definition of reduced frequency becomes

$$k = \frac{\omega b}{(1 + \mu)\Omega r} . \quad (85)$$

The Biot-Savart Theorem is used with wakes extending out to infinity. Since freestream velocity at any point on the rotor blade is a function of both blade section radius and azimuth position, the shed vorticity will experience a build-up and decay as azimuth varies from 0° to 360° . Shipman and Wood developed a decay function to account for the variation in vorticity and incorporate this function and the advance ratio into the integral downwash equation. The pressure distribution is found by applying Söhngen's inversion formula [Ref. 14] to the downwash equation. The pressure distribution is shown to be in the same form as Theodorsen and Loewy, and a modified lift deficiency function is defined to account for the differences. Since this modified lift deficiency function includes Loewy's wake weighting function as one of its terms, the finite wake weighting function could be directly substituted into Shipman

and Wood's lift deficiency function. If the segment of the wake weighting function due to the vorticity decay (ΔW) is modified to account for a finite number of wakes instead of an infinite number, a new finite wake forward airspeed lift deficiency function can be defined, and the remainder of the problem is the same as Shipman and Wood.

2. Compressibility Effects

Adding the effects of compressibility to the rotary wing unsteady aerodynamic problem was first accomplished by Jones and Rao [Ref. 5]. Hammond [Ref. 6] provided an alternate approach to the problem shortly after Jones and Rao, but only the method by Jones and Rao will be presented here.

Jones and Rao expand on Loewy's work by taking the known solution to the fixed wing two-dimensional unsteady airfoil theory and modifying it to include the effect of an infinite number of wakes below the reference airfoil (or rotor disk). Euler's equation is used with a coordinate change to determine the downwash equation. An interesting result is found, and that is for a given circulation, the downwash due to an infinite system of wakes is the same for compressible and incompressible flow. In other words, the circulation generated by layers of shed vorticity beneath an airfoil is independent of Mach number. This fact will be true whether there is an infinite number of wakes or a finite number of wakes. Thus, the finite wake theory can be applied here, and the remainder of the problem is the same as Jones and Rao.

3. NPS Unsteady Panel Code

The NPS Unsteady Panel Code was written by Pang [Ref. 7] to solve the potential flow for two airfoils executing unsteady motion in an inviscid, incompressible flow. In this code, the two airfoil surfaces are approximated by a large number of surface elements, and a uniform source distribution and vorticity are placed on each element. The source strength varies from element to element, while the vortex strength is the same for all elements. The singularity strengths are determined from the flow tangency condition on both airfoil surfaces and the two Kutta conditions.

Extensive comparisons of this code with Theodorsen was accomplished by Riemer [Ref. 17], and the code (using an NACA 0007 airfoil) shows very good agreement with flat plate theory. Comparison of this code with Loewy could not be accomplished easily since it would require a very large number of airfoils to generate the infinite number of wakes. Using the finite wake theory, the code could easily be compared to the case of a single wake. A comparison for pure plunge [Ref. 8] with $h = 2.0$, $k = 0.1234$, and $\bar{h}_0 = 0.14$ are presented in Figure 23. The results show that the NPS Panel Code has very good agreement with the finite wake theory.

B. HIGHER HARMONIC CONTROL

Higher Harmonic Control (HHC) is an active vibration control system for helicopters. The concept of HHC is to alter the aerodynamic loads on the rotor blades such that the blade response is reduced, which in turn reduces the vibratory forces and

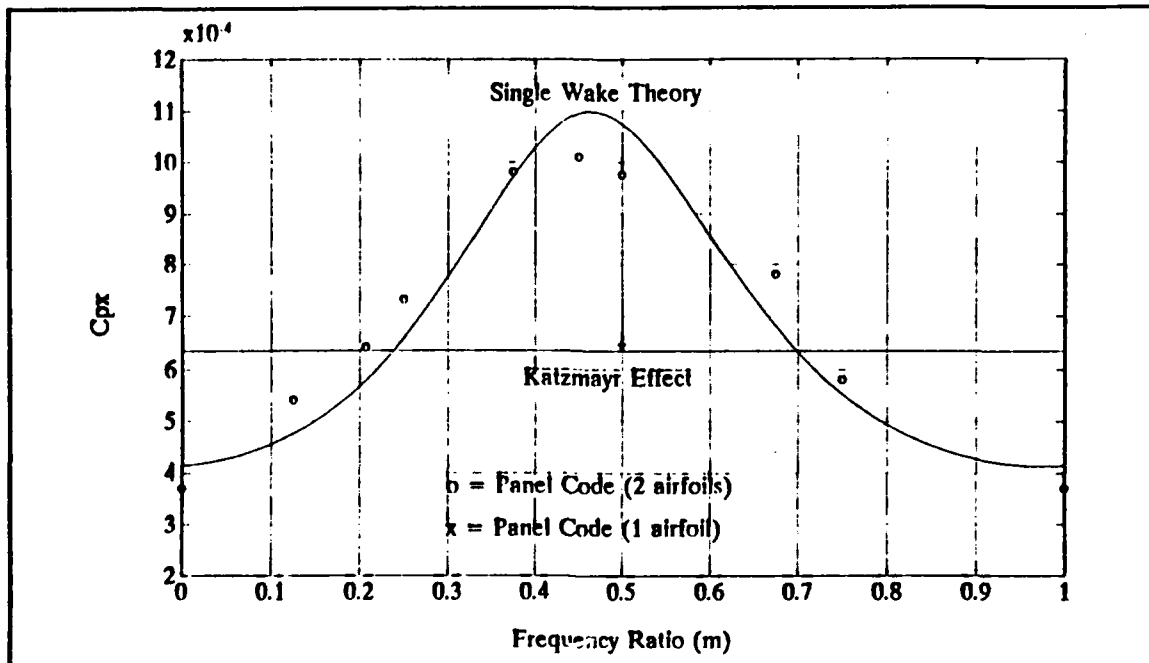


Figure 23. Comparison of propulsive force coefficient in pure plunge ($h = 2.0$, $k = 0.1234$, and $\bar{h}_o = 0.14$).

moments acting at the hub that cause vibration. HHC flight test results [Ref. 15], under a joint NASA-Army sponsored program using a modified OH-6A, show a reduction of airframe vibrations up to 90 percent. Basically, HHC is an electronic, computer-controlled active vibration suppression system which senses and cancels vibrations in a helicopter by Q per revolution feathering or pitch motion of the rotor blades, where Q is the number of rotor blades.⁵ On the OH-6A, higher harmonic blade pitch control was achieved by superimposing 4/rev (or 4P) swashplate motion on basic cyclic and collective control inputs. The aircraft was flown from hover to 100 knots, but the remainder of the discussion will focus on the hover performance.

⁵Normally for helicopters, N is used to represent the number of blades, but to remain consistent with Chapter III Q will be used.

In addition to reducing vibration levels HHC on the OH-6A showed the potential for decreased helicopter power requirements. Figures 24 and 25 show hover power required for three different schedules of HHC open loop excitation. What is of interest here is that the amount of power reduction achieved (on the order of 10% or 20 horsepower) appears to be relatively independent of the type of excitation applied. This power reduction is important, especially in hover where power required is large, because of the benefit of lowering fuel consumption, which can be translated into a larger payload or increased mission time.

The physics behind HHC can be explained by unsteady aerodynamics. The input by HHC to the rotor blade is a pitch oscillation, $\pm 1/3$ degree on the OH-6A. From Figure 10 (infinite wakes) it can be seen that the propulsive force coefficient is negative (drag) for the wake spacing of the OH-6A ($h = 2.0$) regardless of the phasing of the wakes (m). Thus, it might be concluded that pitch oscillations alone cannot account for the substantial reduction of power recorded by the flight tests. If it is assumed that viscous interaction of vortices reduce the problem to a finite wake solution as shown in Figures 17 and 21, the propulsive force obtained is still not sufficient to account for the power reduction even if the wakes were optimally phased.

As stated earlier, HHC provided a 4P pitch input in both collective and cyclic were applied at the blade root. The collective input results in a 4P oscillation along the blade, while the cyclic input results in 3P and 5P oscillations along the blade. From the Southwell plot of the OH-6A [Ref. 16] shown in Figure 26, it can be seen that the second flapwise and third flapwise natural frequencies occur near 3P and 5P

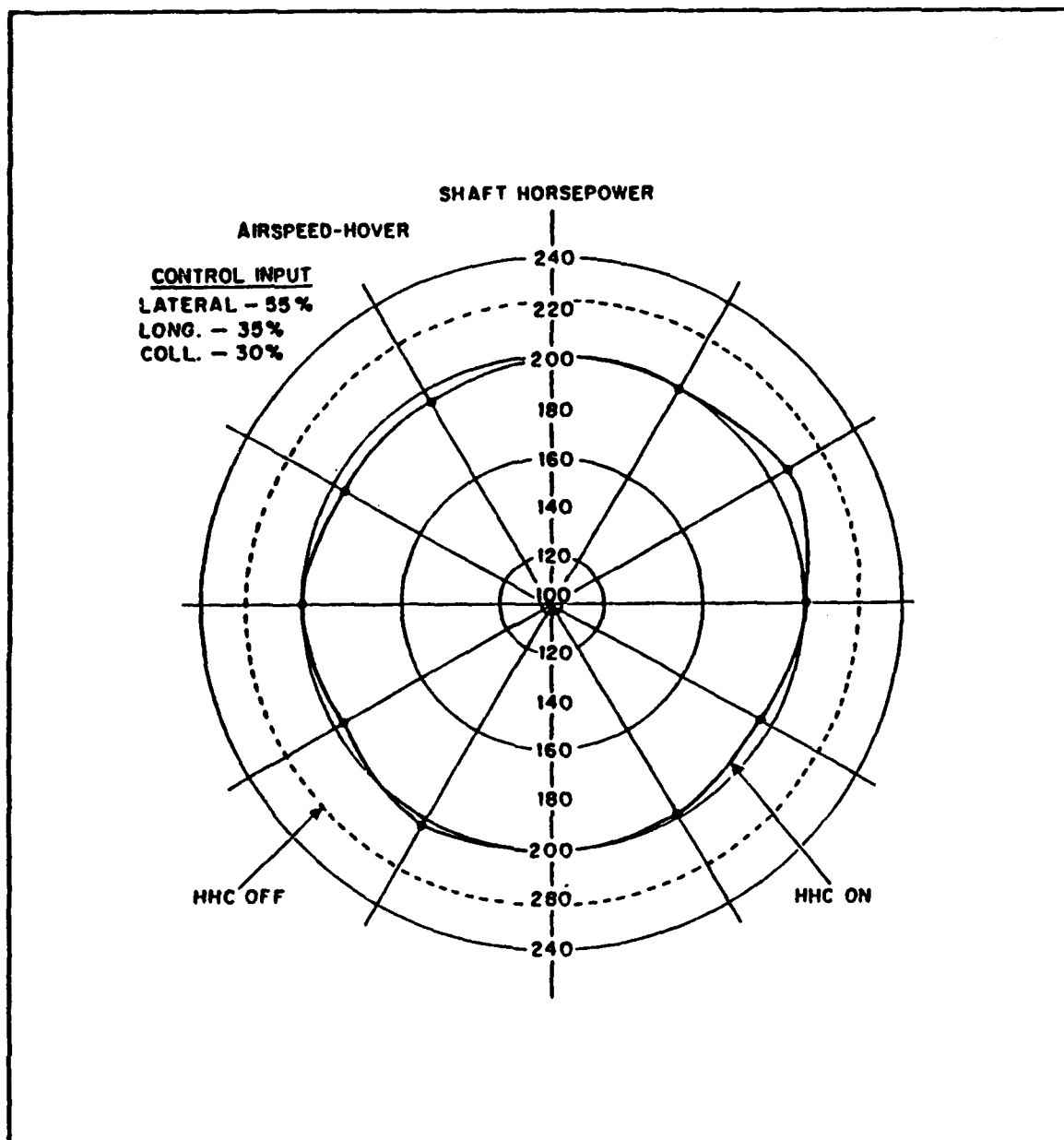


Figure 24. Effect of HHC on main rotor shaft power in hover for selected set of three open loop inputs.

respectively. During the course of a revolution of a blade about the hub, the blade will naturally experience flapping motion due to changes in angle of attack, or pitch changes, as the blade proceeds around. Since 3P and 5P flapping frequencies are

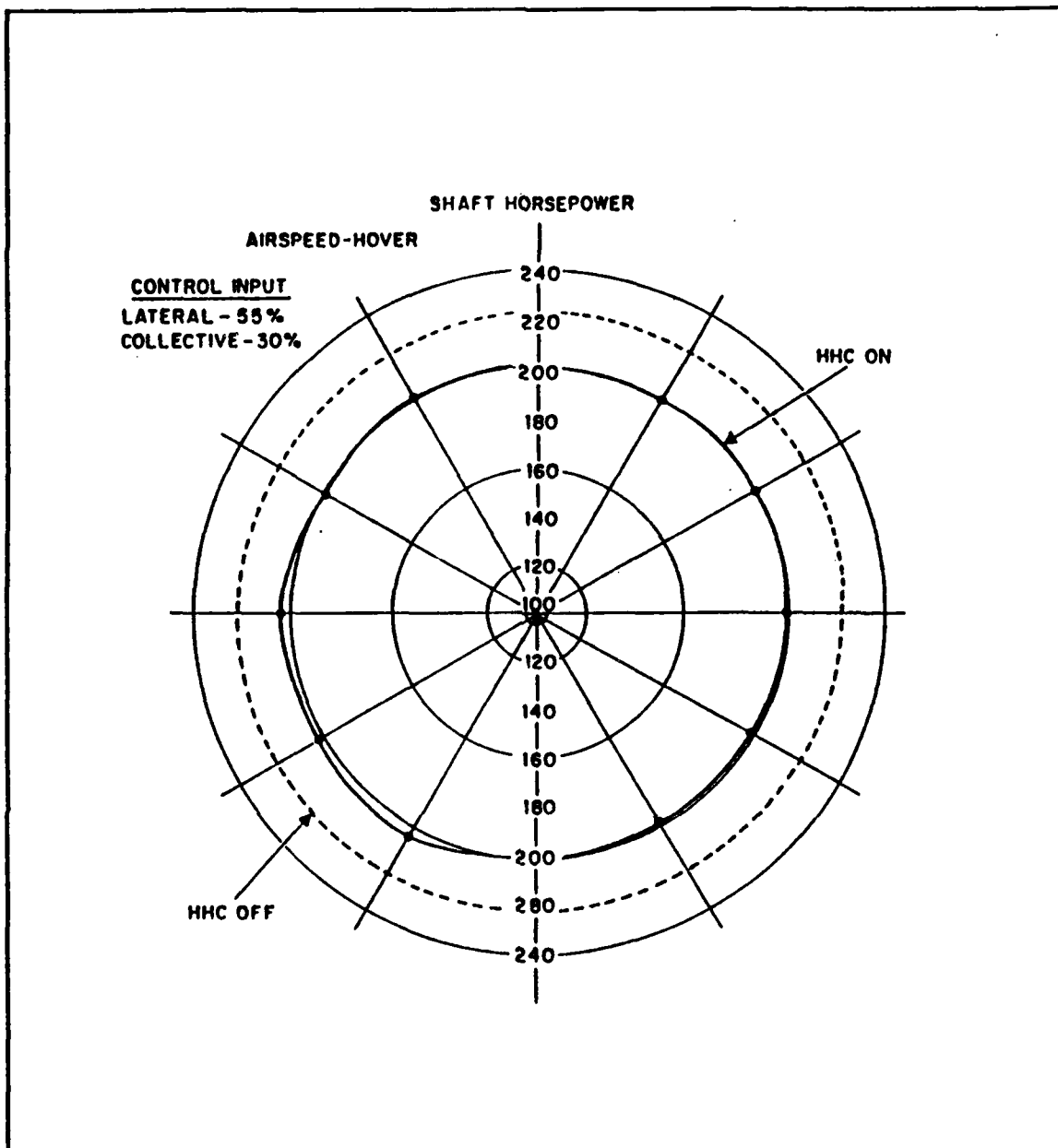


Figure 25. Effect of HHC on main rotor shaft power in hover for selected set of two open loop inputs.

near natural frequencies, small 3P and 5P pitch inputs will result in much greater flapping outputs. Thus, the unsteady aerodynamics of HHC for the OH-6A is coupled pitch-plunge oscillations. Figures 11, 18, and 22 show that coupled pitch-plunge

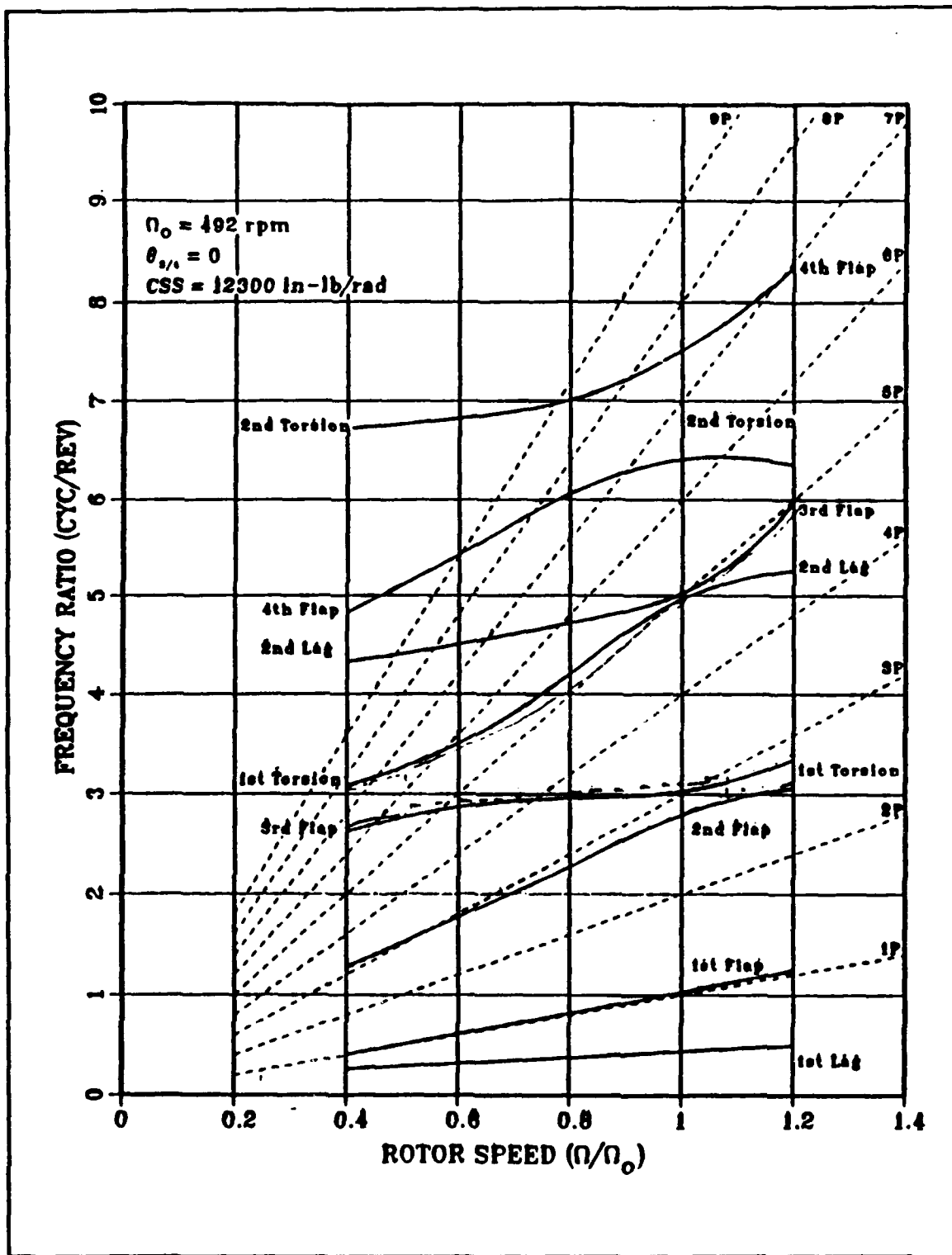


Figure 26. Southwell plot of the OH-6A rotor blade.

oscillations always result in a propulsive force regardless of the number of wakes considered or phasing of those wakes. What is of greater importance is that if the wakes are optimally phased together, the propulsive force is an order of magnitude higher than pure plunge or pure pitch. The bottom line for the OH-6A is that the inherent natural frequencies of the blades along with 4P cyclic inputs result in coupled pitch-plunge oscillations which yield a propulsive force large enough to account for a substantial power reduction for the helicopter.

V. CONCLUSION

The unsteady aerodynamics of rotary wings is inherently more complicated because of the layers of shed vorticity, or wakes, beneath the rotor disk that interact with the rotor blades. The Biot-Savart Theorem is used to account for the effects of these wakes, and a modified lift deficiency function is developed for use with Theodorsen's equations of motion [Ref. 1]. Loewy [Ref. 2] develops a lift deficiency function for the case of an infinite number of wakes, while this thesis develops a lift deficiency function for any finite number of wakes. This thesis also presents the special case of a single wake, and shows that for small wake spacings there are certain reduced frequencies where the lift is actually enhanced. In other words, the lift deficiency function becomes a lift efficiency function.

The equations describing the propulsive force generated by an oscillating airfoil are developed by Garrick [Ref. 3]. These equations are derived from Theodorsen's equations of motion, and included the lift deficiency function as a parameter. Since the rotary wing lift deficiency functions (Loewy's and the finite wake) are just modifications of Theodorsen's work, Garrick's work can be applied to rotary wing unsteady aerodynamics. When either Loewy's lift deficiency function or the finite wake lift deficiency function is used, the propulsive force can be greatly enhanced with the proper phase relationship of the wakes. The use of coupled pitch and plunge can result in a propulsive force which is an order of magnitude higher than either pure

plunge or pure pitch. This coupling of plunge and pitch is used to explain the performance benefits reported in the flight test data for the OH-6A equipped with Higher Harmonic Control. Coupled pitch-plunge oscillations with proper phase relationships of the wakes yield a propulsive force large enough to account for a substantial power reduction for the helicopter.

APPENDIX A

I. FLIGHT OF THE HUMMINGBIRD

For thousands of years, man has been intrigued by the flight of birds. Early Greek mythology includes a tale of Daedalus and Icarus who made wings held together by wax, and escaped their imprisonment on the island of Crete by flying through the air like birds. Early attempts by man to fly were usually designed around imitations of birds. Most of these early attempts met disastrous results because of a lack of clear understanding of the aerodynamics of ornithological flight, and that is the wing on a bird is a coupled lift and propulsion device. In fact, the Wright brothers first successful flight demonstrated man's limited knowledge of aerodynamics by decoupling lift and propulsion in order to achieve flight. To this day lift and propulsion remain decoupled.

The coupling of lift and propulsion in birds can be explained by unsteady aerodynamics. As a bird flaps its wing down, the trailing edge also begins to rise [Ref. 18]. Thus, the motion of the wing is a coupled pitch-plunge motion. It was shown earlier that coupled pitch-plunge motion yields a propulsive force that is an order of magnitude higher than pure plunge. Since most birds require some forward airspeed before being capable of achieving flight and the rate of flapping is between 1 to 5 beats per second, the analogy to unsteady aerodynamics can be described by Garrick's equation for coupled pitch-plunge using Theodorsen's lift deficiency function

(equation (36)). Birds take advantage of the extra propulsive benefit of coupled pitch-plunge to make flight appear effortlessly.

A few birds, most notably the hummingbirds, are capable of hovering. In hovering flight the hummingbird's body is angled upward at about 45° , so that the plane of wing flapping is approximately horizontal. As the wing moves up (backward) and down (forward), the angle of attack, or pitch, changes making a figure eight pattern that is on its side. In essence, the hummingbirds wing motion is similar to the motion of the hands of a swimmer when he is treading water. Once again the hummingbird takes advantage of a coupled pitch-plunge motion to achieve a higher propulsive force.

What is unique about the hummingbird is the rate of flapping, or the oscillation frequency; it is on the order of 40 to 80 beats per second. Welty [Ref. 18] states that the hovering flight of the hummingbird is grossly inefficient when compared to helicopter rotor blades, but this is overcome by an increase in apparent velocity created by trailing currents from the previous reverse stroke. This is not exactly correct. The hummingbird's wing motion is similar to that of helicopter rotor blades. Both are cyclic motions of changes in pitch (angle of attack) and plunge (flapping). The hummingbird is just as efficient as a helicopter - both have a large power required in hover. The apparent increase in velocity can be explained by trailing vortices. Since the hummingbird's rate of flapping is large in a hover, the wake created by a previous stroke will not dissipate and be carried downstream. Each stroke of the wing always has layers of shed vorticity directly below it. If these wakes are optimally phased depending on the number of wakes, the benefit will be a propulsive force

greater than that of non-hovering birds. The hummingbird must use wakes efficiently, or it will not hover. Thus, the analogy of the hummingbird to unsteady aerodynamics can be described by Garrick's equation for coupled pitch-plunge using the finite wake lift deficiency function, or in the case of a pure hover Loewy's lift deficiency function.

LIST OF REFERENCES

1. Theodorsen, T., "General Theory of Aerodynamic Instability and the Mechanism of Flutter," *NACA T.R. No. 496*, 1935.
2. Loewy, R. G., "A Two-Dimensional Approximation to the Unsteady Aerodynamics of Rotary Wings," *Journal of the Aeronautical Sciences*, Vol. 24, No. 2, pp. 81-92, February 1957.
3. Garrick, I. E., "Propulsion of a Flapping and Oscillating Airfoil," *NACA T. R. No. 567*, 1936.
4. Shipman, K. W., and Wood, E. R., "A Two-Dimensional Theory for Rotor Blade Flutter in Forward Flight," *Journal of Aircraft*, Vol. 8, No. 12, pp. 1008-1015, December 1971.
5. Jones, W. P., and Rao, B. M., "Compressibility Effects on Oscillating Rotor Blades in Hovering Flight," *AIAA Journal*, Vol 8, No. 2, pp.321-329, February 1970.
6. Hammond, C. E., "Compressibility Effects in Helicopter Rotor Blade Flutter," Ph. D. Thesis, Georgia Institute of Technology, Atlanta, Georgia, December 1969.
7. Pang, K. C., "A Computer Code (USPOTF2) for Unsteady Incompressible Flow Past Two Airfoils," Master's Thesis, Naval Postgraduate School, Monterey, California, September 1988.
8. Wood, E. R., Platzer, M. F., Abouahma, A., Couch, M. A., "On The Unsteady Aerodynamics of Higher Harmonic Control," paper presented at Nineteenth European Rotorcraft Forum, Cernobbio (Como), Italy, 14-16 September 1993.
9. Scanlan, R. H., and Rosenbaum, R., *Introduction to the Study of Aircraft Vibration and Flutter*, pp.379-400. The MacMillan Company, New York, 1951.
10. Katzmayr, R., "Effect of Periodic Changes of Angles of Attack on Behavior of Airfoils," *NACA T. M. No. 147*, October 1922.
11. Richardson, E. G., "The Physical Aspects of Fish Locomotion," *Journal of Experimental Biology*, Vol. III, No. 1, pp. 63-74, 1936.

12. von Karman, T., and Burgers, J. M., "General Aerodynamic Theory - Perfect Fluids," *Aerodynamic Theory*, Durand, W. F., ed., Vol. II, Julius Springer (Berlin), 1935.
13. Donovan, A. F., and Lawrence, H. R., *Aerodynamic Components of Aircraft at High Speeds*, p. 706, Princeton University Press, Princeton, New Jersey, 1957.
14. Söhngen, H., "Die Lösungen der Integralgleichung und deren Anwendung in der Tragflugeltheorie," *Mathematische Zeitschrift*, Band 45, 1935.
15. Wood, E. R., Powers, R. W., Cline, J. H., and Hammond, C. E., "On Developing and Flight Testing a Higher Harmonic Control System," *Journal of the American Helicopter Society*, Vol. 30, No. 2, January 1985.
16. Wood, E. R., Higman, J., and Kolar, R., "Higher Harmonic Control Promises Improved Dynamic Interface Operations," paper presented at AGARD Proceedings of the 78th Flight Mechanics Panel, Seville, Spain, 20-23 May 1991.
17. Riester, P. J., "A Computational and Experimental Investigation of Incompressible Oscillatory Airfoil Flow and Flutter Problems," Master's Thesis, Naval Postgraduate School, Monterey, California, June 1993.
18. Welty, J. C., *The Life of Birds*, 3d ed., pp. 536-539, Saunders College Publishing, Philadelphia, 1982.

INITIAL DISTRIBUTION LIST

1. Defense Technical Information Center 2
 Cameron Station
 Alexandria, VA 22304-6145

2. Superintendent 2
 Attn: Library, Code 1424
 Naval Postgraduate School
 Monterey, CA 93943-5000

3. Chairman, Code AA/CO 1
 Naval Postgraduate School
 Monterey, CA 93943-5000

4. Dr. E. Roberts Wood 4
 Dept. of Aeronautics and Astronautics, Code AA/Wd
 Naval Postgraduate School
 Monterey, CA 93943-5000

5. Dr. Max F. Platzer 3
 Dept. of Aeronautics and Astronautics, Code AA/Pl
 Naval Postgraduate School
 Monterey, CA 93943-5000

6. LTC Ahmed Abourahma 1
 Dept. of Aeronautics and Astronautics
 Naval Postgraduate School
 Monterey, CA 93943-5000

7. LT Mark A. Couch 2
 508 Sawgrass Ct.
 Lee's Summit, MO 64064